Supporting Information

Predictive Minisci and P450 Late Stage Functionalization with Transfer Learning

Emma King-Smith, Felix A. Faber, Usa Reilly, Anton V. Sinistkiy, Qingyi Yang, Bo Liu, Dennis Hyek, and Alpha A. Lee*

Correspondence to: aal44@cam.ac.uk

Table of Contents

General Materials and Methods:[1]

Unless otherwise noted, all chemicals and reagents for chemical reactions were purchased at the highest commercial quality and used without further purification. Liver microsomes were purchased from the following vendors: female mouse, male rat, male cynomolgus monkey and non-transfected microsomes (Corning, Woburn, MA); dexamethasone- induced male rat, male hamster, male dog and pooled male & female human (prepared in-house at Pfizer, Groton, CT); and male guinea pig and male rabbit (Xenotech, Lenexa, KS). Note, human and monkey liver microsomes are considered biohazardous materials and appropriate precautions should be taken during handling and disposal. Recombinant human P450 enzymes heterologously expressed in microsomes from Sf9 cells were custom prepared by Panvera (Madison, WI).

Code:

The pipeline, modules, and trained models can be found at https://github.com/emmaking-smith/SET_LSF_CODE.

Liver Microsomes and Recombinant CYP Enzyme Screen Procedure:

Loratadine (20.0 μM, 10.0 nmol) was incubated with 9 mammalian liver microsomes (2.0 mg/mL) and 9 human recombinant P450 enzymes (2.0 mg/mL). The total volume in each well was 0.5 mL which contained potassium phosphate buffer (0.1 M, pH 7.4), MgCl2 (3.3 mM, 1.65 μmol) and acetonitrile (0.4% v/v). The reaction was initiated with the addition of NADPH (1.3 mM, 0.65 μmol) and agitated at 37 ˚C in a reciprocal shaking bath at 1" throw for 1 hour. The incubation was quenched with the addition of acetonitrile (1.5 mL), followed by centrifugation (1700 g, 5 min). The supernatant was removed and the solvent reduced using a Genevac centrifuge evaporator. The residue was reconstituted in 0.1 mL of 1% formic acid in H2O / 20% acetonitrile, followed by centrifugation (1700 g, 5 min). The samples were analyzed using the General HPLC-MS Method for Screen Analysis.

Biomimetic Metalloporphyrin Oxidation (BMO) Screen Procedure:

A high throughput BMO screen was completed on a miniature scale, examining the key variables of metalloporphyrin, oxidant and solvent. Nine different metalloporphyrins plus control without metalloporphyrin, six oxidants and two solvents were screened in a matrix of 120 combinations. The remaining variables were held constant according to the standard protocol described below.

The reactions were set-up in two 96-well arrays using miniature 8 x 20 mm (0.2 mL) glass vials under standard glove box conditions (H_2O and O_2 <20 ppm). A 8 x 20 mm (0.2 mL) glass vial equipped with stir bar was dispensed the reaction solvent (100 μL, 4.0 mM) followed by a solution of 1 (5.0 μL, 0.4 μmol), added as a 0.1 M solution in dichloroethane. Stirring was initiated before the metalloporphyrin (4.0 μL, 0.04 μmol) was charged, as a 10.0 mM solution in dichloroethane. The vial was treated with a 0.1 M solution of imidazole (2.4 mL, 0.24 μmol) in H_2O, followed by a 0.4 M solution of formic acid (4.0 μL, 0.16 μmol) in H_2O. Finally, the oxidant (8.0 μL, 0.08 μmol) was added as a 0.1 M solution in dichloroethane. The reaction vial

was crimp sealed with a PTFE / Silicone / PTFE septa to the glove box environment before the reaction was left to stir at 25 ˚C for 18 hours. After this time period, the reaction was diluted with acetonitrile (0.2 mL) and analyzed directly by UPLC/MS. The UPLC/MS method used a 0.1% AcOH / NH_4CO2H / H_2O gradient over 0.8 minutes, running from 5-95% acetonitrile using a Waters Acquity UPLC BEH C18 30 x 2.1 mm column at 100 ˚C with a flow rate of 2.5 mL/min and a detection wavelength of 210-360 nm. 0.5 µL injections were made directly from diluted reaction mixtures and ionization monitored in positive mode.

General Minisci Functionalization with Baran Diversinates™ Procedure:

To 1-dram pressure release vial containing Diversinate™ sulfinate reagent as sodium or zinc salts e.g., RSO_2Na or $(RSO_2)_2Zn$ (3 eq - 6eq), was added to a solution of the test substrate molecule (~2 µmol, 1 eq) in DMSO (~70-100 µL, 30 mM) and TFA (4 eq) followed by *tert*-butyl hydroperoxide, 70% in water (5 eq) at room temperature. The resulting reaction mixture was capped and heated to 50 ˚C overnight. The crude reaction mixture was dissolved in 3:1 acidic mobile phase (1% acetonitrile, 0.1% formic acid) and acetonitrile (~3 mL) then purified via HPLC (XSelect 5 µm C18 130 Å, 250 x 10 mm @ 2 mL/min). The respective fractions were pooled, and solvent removed using the EZ-2 Elite Genevac (3-hour HPLC setting, 34 ˚C / 238 mbar to 41 ˚C / 7 mbar). Each isolate was characterized by MS and NMR. Due to the low amounts of isolates generated, gravimetric mass analysis is not possible; qNMR in conjunction with the enhanced sensitivity using a 1.7 mm micro-cryoprobe in DMSO-d_6 solvent was used to determine the concentration of the sample.

General Minisci Functionalization with Molander BF_3K Salts Procedure:

To 1-dram pressure release vial containing the test substrate molecule (~2 µmol, 1 eq), potassium trifluoroborate salt of the radical (1.5 - 2 eq), in a 1:1 mixture of acetic acid and water to make a 30 mM solution and $Mn(OAc)_3$ was added in one portion. The resulting reaction mixture was capped and heated to 50 ˚C overnight. The crude reaction mixture was dissolved in 3 :1 acidic mobile phase (1% acetonitrile, 0.1% formic acid) and acetonitrile (~3 mL) then purified via HPLC (XSelect 5 µm C18 130 Å, 250 x 10 mm @ 2 mL/min). The respective fractions were pooled, and solvent removed using the EZ-2 Elite Genevac (3-hour HPLC setting, 34 ˚C / 238 mbar to 41 ˚C / 7 mbar). Each isolate was characterized by MS and NMR. Due to the low amounts of isolates generated, gravimetric mass analysis is not possible; qNMR in conjunction with the enhanced sensitivity using a 1.7 mm micro-cryoprobe in DMSO-d_6 solvent was used to determine the concentration of the sample.

Calculating the Fukui Indices:
Reactivity indices for electrophilicity and nucleophilicity for the *i*-th atom were computed by multiplying the corresponding Fukui index [$F_i(+)$ or $F_i(-)$, respectively] of the *i*-th atom by global electrophilicity / nucleophilicity for the given molecule.

Reactivity indices for radical reactions were taken to be equal to the corresponding Fukui indices $F_i(0)$. Global nucleophilicity of the molecule was computed as 8 eV + HOMO, and its global electrophilicity as (HOMO+LUMO)2/(4(LUMO-HOMO)), where HOMO and LUMO are the HOMO and LUMO energies of the molecule.

Fukui indices of the *i*-th atom $F_i(+)$, $F_i(-)$ and $F_i(0)$ were computed as differences between the atomic charge of the *i*-th atom in the original molecule $q_i(N)$ with N electrons, the charge of the same atom after adding one electron to the molecule $q_i(N+1)$, and the charge of the same atom after removing one electron from the molecule $q_i(N-1)$:

$F_i(+) = q_i(N) - q_i(N+1)$
$F_i(-) = q_i(N-1) - q_i(N)$
$F_i(0) = [q_i(N-1) - q_i(N+1)]/2$

For electrophilicity and radical indices, quantum chemical computations were run with PBE/6-311G, and for nucleophilicity with B3LYP/6-311G**. As partial atomic charges, Mulliken charges were used. These DFT functionals, basis sets and types of atomic charges were chosen by optimizing the predicting performance of the reactivity indices in S_NAr and EAS reactions of an internal dataset of small organic molecules (unpublished). Quantum chemical computations were run in Terachem.[2]

Tie Breakers for F-scores:

Whilst F-scores represented an excellent first pass, it did lead to degenerate best models for a variety of loss function weightings. We thus developed our own in-house metric, EKS metric, that was more discerning than the F-score. Like the F-score, this metric would provide a single number encompassing model accuracy and precision but would be more penalizing towards errors, elucidating model performance differences more easily (Figure S1 & S2). It would also address the challenge of accurate baselines when evaluating model performance. A model that predicts nothing reacts would receive and F-score of 0, and a model that predicts everything reacts would receive a non-negative score (Eq. S1). This is slightly unintuitive, as a model that predicts most atoms will not undergo functionalization is actually representing a more chemically correct understanding of reactivity. The most functionalized molecule only saw 30% number of sites reacting, or 70% of its atoms did not react. Indeed, most of the molecules in our dataset saw 1 reaction site of fewer.

Our in-house metric would give a low score if the model yielded a high number of false positives (FP) or false negatives (FN) and a high score if the model yielded a high number of true positives (TP) or true negatives (TN). The score should also be dependent upon the scarcity of predicted reactive sites. The value of each TP and TN should be dependent on the how frequently the model predicts positives and negatives, respectively. An overly cautious model which blindly guesses that all atoms are unreactive should receive a lower value for each TN it predicts compared to a model that is more judicious about its unreactive predictions. To this end, the following metric was used (Eq. S2). The variables, $pred_p$ and $true_p$ refer to the ratio of predicted positives to all reactive sites. A $pred_p$ of 1 indicates a model that predicts all sites react and a $pred_p$ of 0 indicates a model where every molecule is unreactive. As reference, on the retrospective test set, a perfect model would receive a score of 119, a model that predicts nothing reacts would receive a score of -1.83, and a model that predicts everything reacts would be given a score of -1455. If a prediction is only 3% incorrect, the model score drops to 72, and at only 5% incorrect the score becomes 46.5.

Equations:

Eq. S1: $$\text{F-score} = \frac{2 \cdot \text{TP}}{2 \cdot \text{TP} + \text{FP} + \text{FN}}$$

Eq. S2: $$\begin{aligned}\text{score} = \ & \text{FP} \cdot \log(true_p) + \text{FN} \cdot \log(1 - true_p) \\ & - \text{TP} \cdot \log(pred_p) - \text{TN} \cdot \log(1 - pred_p)\end{aligned}$$

Eq. S3: $$\text{BCE Loss} = \sum_{i=0}^{n} w_i \cdot (y_i \cdot \log(x_i) + (1 - y_i) \cdot \log(1 - x_i))$$

Eq. S4: $$\begin{aligned}\text{BCE weight 1} = \ & x \cdot y \cdot \log(pred_p) + (1 - y) \cdot (1 - x) \cdot \log(1 - pred_p) \\ & + (1 - y) \cdot x \cdot \log(true_p) + y \cdot (1 - x) \cdot \log(1 - true_p)\end{aligned}$$

Eq. S5: $$\begin{aligned}\text{BCE weight 2} = \ & [x \cdot y \cdot \log(pred_p) + (1 - y) \cdot (1 - x) \cdot \log(1 - pred_p) \\ & + (1 - y) \cdot x \cdot \log(true_p) + y \cdot (1 - x) \cdot \log(1 - true_p)] \\ & + [y \cdot x \log(true_p) + (1 - y) \cdot (1 - x) \cdot \log(1 - true_p) \\ & + (1 - y) \cdot x \cdot \log(1 - pred_p) + y \cdot x \cdot \log(pred_p)]\end{aligned}$$

Eq. S6: $$\begin{aligned}\text{BCE weight 3} = \ & [x \cdot y \cdot \log(pred_p) + (1 - y) \cdot (1 - x) \cdot \log(1 - pred_p) \\ & + (1 - y) \cdot x \cdot \log(true_p) + y \cdot (1 - x) \cdot \log(1 - true_p)] \\ & + 2 \cdot [y \cdot x \log(true_p) + (1 - y) \cdot (1 - x) \cdot \log(1 - true_p) \\ & + (1 - y) \cdot x \cdot \log(1 - pred_p) + y \cdot x \cdot \log(pred_p)]\end{aligned}$$

$x =$ predicted values $w =$ weighting values

$y =$ experimental values, always 0 or 1

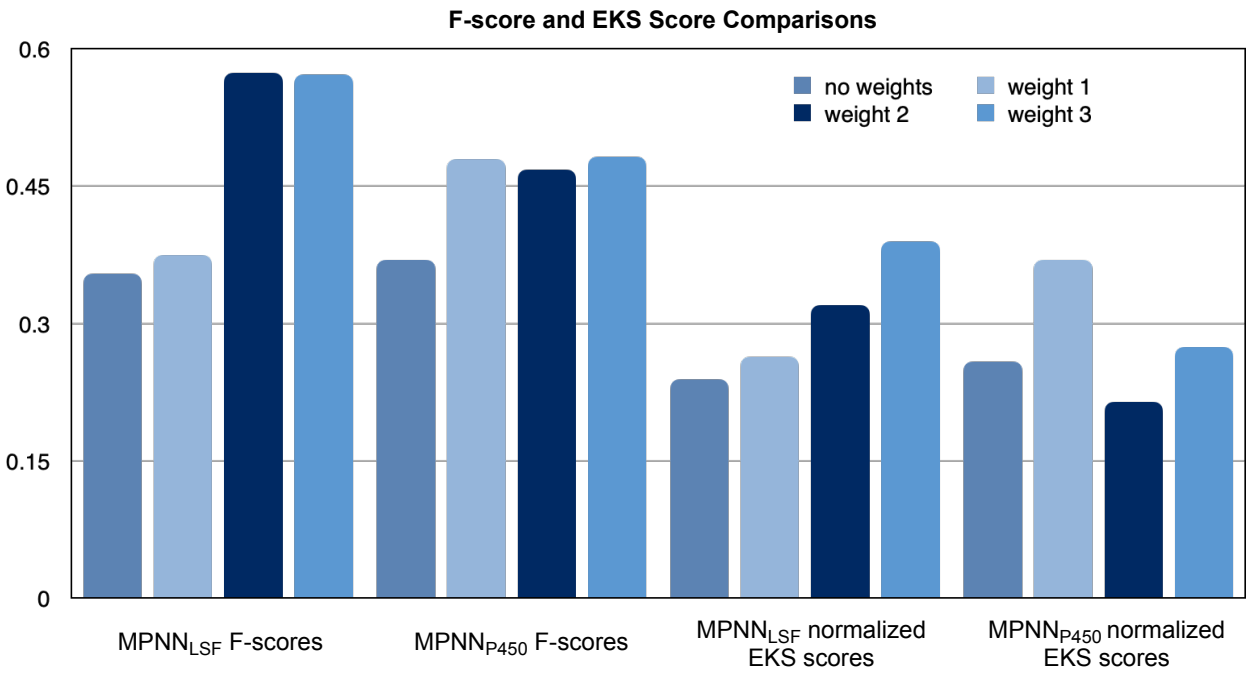

Figure S1: The comparisons of the best models', MPNN$_{LSF}$ and MPNN$_{P450}$, F-scores and normalized EKS scores at various Binary Cross Entropy Loss weightings on the retrospective and P450-only test set respectively. Notice that the normalized EKS scores show more discernment in model performance between different weightings. Weight 2 for MPNN$_{LSF}$ has a nearly identical F-score with weight 3, but EKS scores show a significant edge to weight 3.

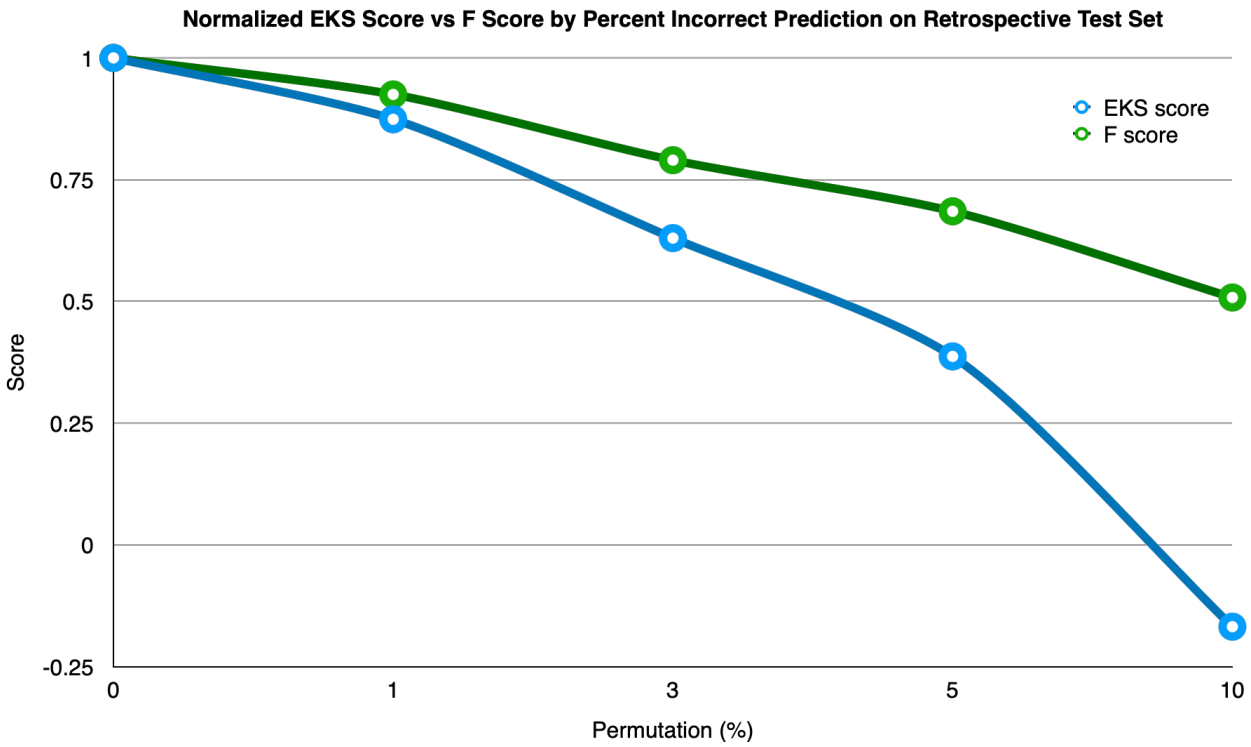

Figure S2: Comparison of sensitivity of incorrect predictions between EKS score and F-score. Analysis performed on the retrospective test set.

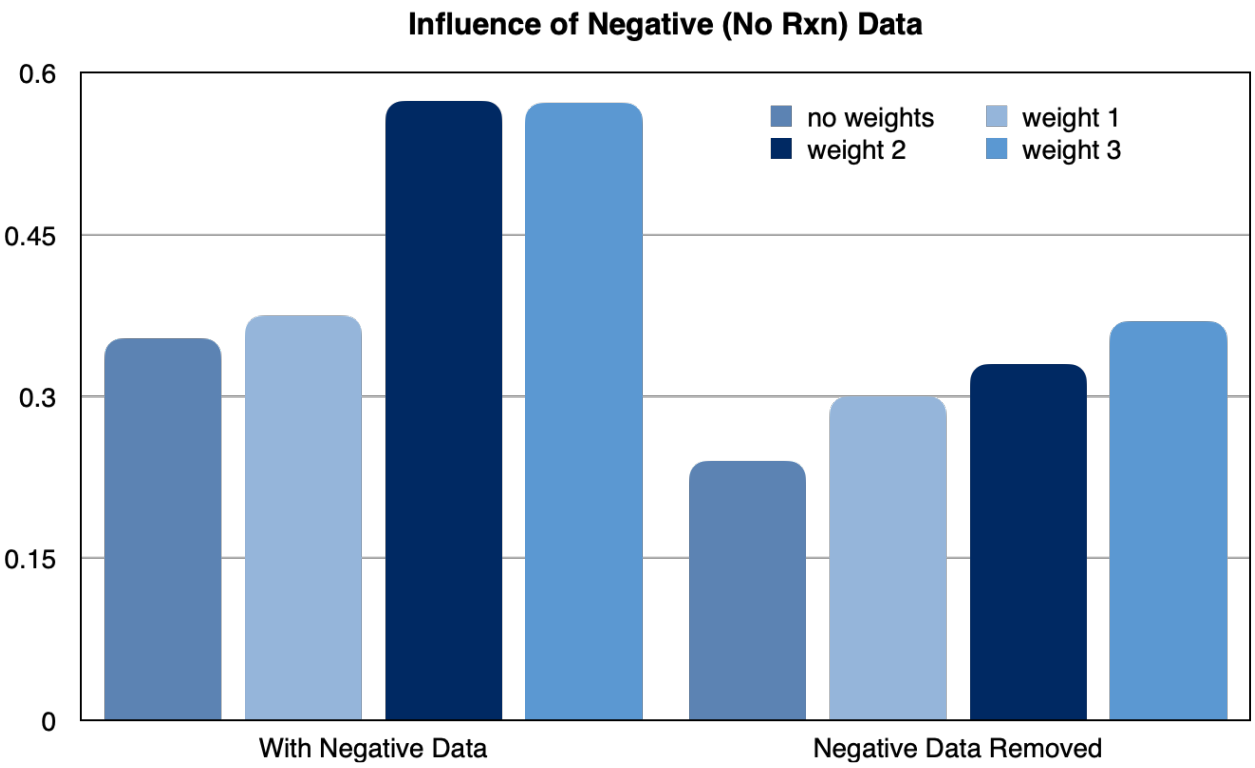

Figure S3: The effect of removing datapoints that saw no reaction.

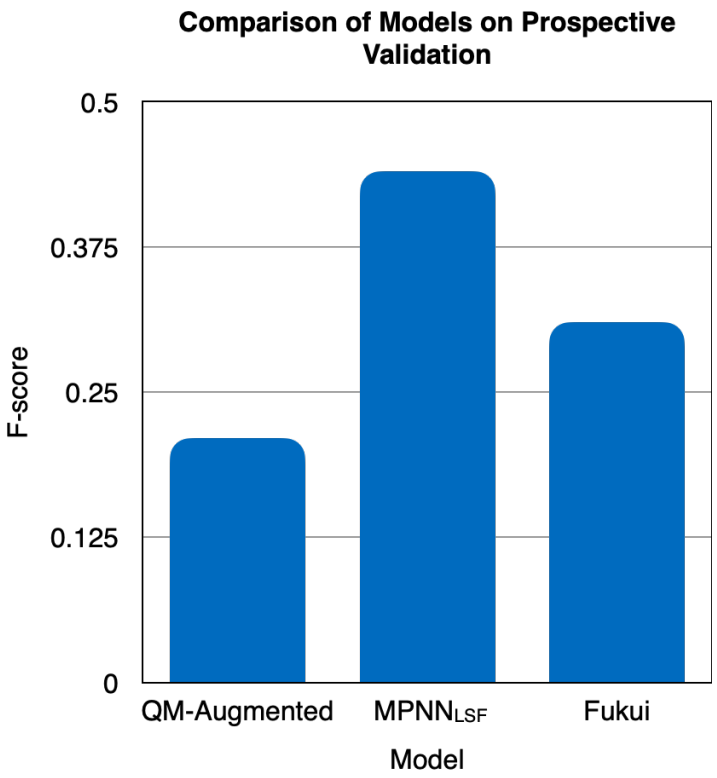

Figure S4: Comparison of $MPNN_{LSF}$ to QM-augmented MPNN (molecular dynamics simulations on atomic density representations).

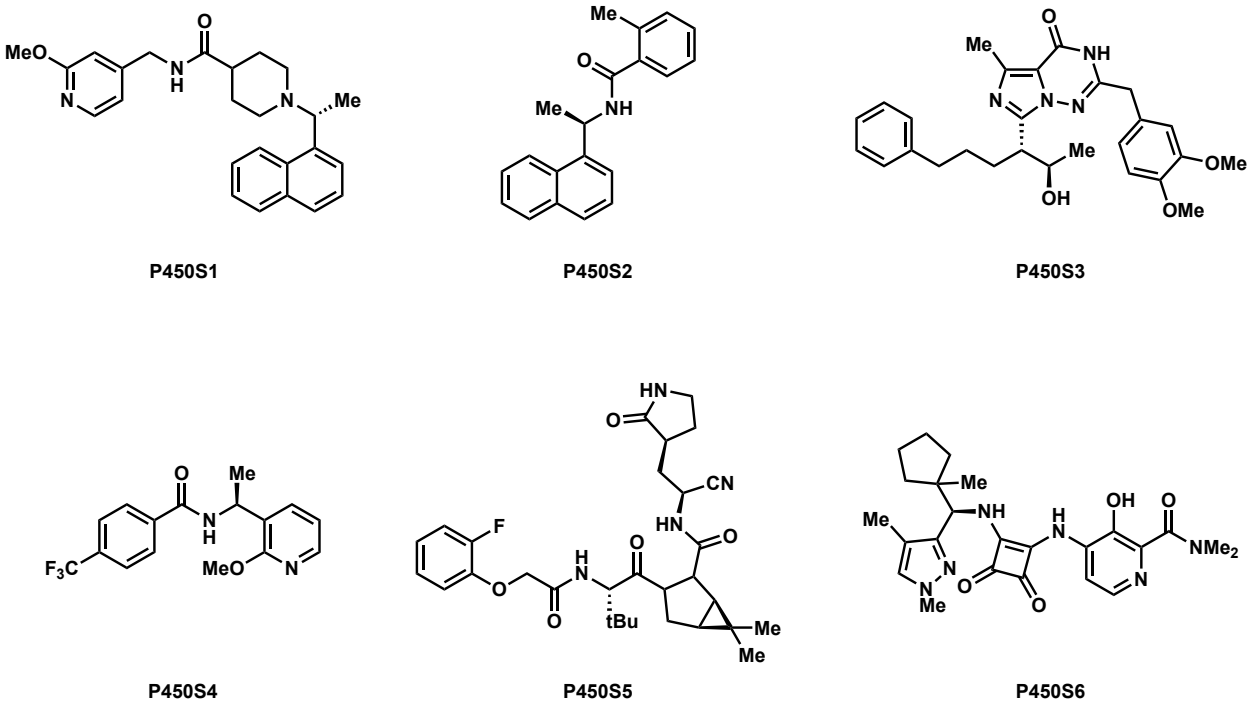

Figure S5: Representative molecules in the P450-only test set.

Table S1: Unique Reaction Conditions

Reagents	***Reagents (Cont.)***	***Acids***	***Additives***	***Solvents***
O_2	$NH(Boc)CH_2BF_3K$	None	None	K phosphate
$(CF_3SO_2)_2Zn$	N-methyl acetamide	TFA	$FeSO_4$	buffer
$(HCF_2SO_2)_2Zn$	glycine	AcOH	pyridine N-	DMSO
$MeOCH_2BF_3K$	1-pyrrolidine-Me-BF_3K	H_2SO_4	oxide	DMSO/H_2O
N-Me formamide	iodo methylnitrile	HCl	$AgNO_3$	AcOH/ H_2O
$HOCH_2SO_2Na$	N,N-diMeCH_2BF_3K	AcOH/H_2O	dicumyl	MeCN
DAST	c$PrCO_2H$	TFA/AcOH/H_2O	peroxide	DCM
Selectfluor	2-CH_3c$PrSO_2Na$	TBAF	$NiCl_2$	MeCN/ H_2O
H_2O	BnO-nBu	HBr	benzoyl	TFE
NFSI	$HO(CH_2)_5CO_2Na$		peroxide	H_2O
RBF_3K	$(nPrSO_2)_2Zn$		tBBP	$CHCl_3$
1,2,3-triazole	$AcNHCH_2BF_3K$		$Fe(acac)_3$	None
c$BuBF_3K$	$(FCH_2SO_2)_2Zn$		$Mn(OAc)_3$	benzene
CF_3SO_2Na	$(cHexSO_2)_2Zn$		$FeCl_3$	Et_2carbonate/H_2O
CH_3CO_2H	$(ClCH_2SO_2)_2Zn$		$Fe(NO_3)_3$	acetone
tBuOOAc	PhIO		$FeCl_2$	DCE
$THFSO_2Na$	NaOCl		pyridine	MeOH
iodo-oxetane	2,6-Cl_2PyNO		imidazole	AcOH
MeOH	PIDA		AgF	DMSO/AcOH/
N$BocAzetidineSO_2Na$	mCPBA		NaOH	H_2O
N$BocAzetidineBF_3K$	$[nBu_4N]IO_4$			MeCN/MeOH
iodo NBocAzetidine	$CH_3CF_2SO_2Na$			DCM/H_2O
1-CF_3-c$PrSO_2Na$	NHBoc glycine			DCM/ H_2O
i$PrBF_3K$	HCF_2CO_2H			/DMSO
i$PrCO_2H$	$(CF_3CH_2SO_2)_2Zn$			DCE/ H_2O
N-Chlorosuccinimide	3,3-diF c$BuBF_3K$			/DMSO
$B(OMe)_3$				$PhCF_3$/ H_2O
$CF_3(CH_2)_2SO_2Na$				$CHCl_3$/ H_2O
c$PrBF_3K$				perfluorotoluene/
t$BuBF_3K$				H_2O
4,4-diF				perfluorohexane/
c$HexCH_2BF_3K$				H_2O
4,4-diF c$HexSO_2Na$				DCE/H_2O
c$BuOCH_2BF_3K$				PhOMe/H_2O
c$HexBF_3K$	***Oxidants:***			MeCN/DCM
$THPBF_3K$	NADPH, P450			$CF_3C_6H_5$
c$PrCH_2BF_3K$	TBHP			MeOH/H_2O
pyrazole	$Mn(OAc)_3$			
1,2,4-triazole	$Et_4N \bullet BF_4$			
CBMG	TBADT			
$(iPrSO_2)_2Zn$	$(NH_4)_2S_2O_8$			
c$PrCH_2OCH_2BF_3K$	Ir[dF(CF_3)ppy]$_2$(dtbbpy)][PF_6]			
$CH_3CH_2SO_2Na$	Ir[dFppy]$_3$[PF_6]			
oxetane-BF_3K	$Ru(bpy)_3Cl_2$			
$Et_3N \bullet 3HF$	H_2O_2			
HCF_2SO_2Na	$K_2S_2O_8$			
Pivalic acid	$Cu(OAc)_2$			
N-acetyl glycine	$Pd(OAc)_2$			
N-methyl glycine	$KMnO_4$			
N,N-diemthyl glycine	$Ce(SO_4)_2$			
CF_3BF_3K	$K_2Cr_2O_7$			
	benzoquinone			
	M[TFPP]			

Compound Characterizations:

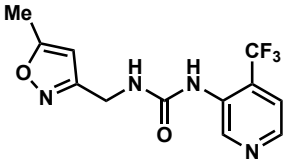

S1

Prepared according to General Minisci Functionalization with Baran Diversinates™ Procedure.

^{1}H NMR (600 MHz, DMSO-d$_6$): δ 9.16 (s, 1H), 8.47 (d, *J* = 2.9 Hz, 1H), 8.22 (s, 1H), 7.66 (d, *J* = 5.1 Hz, 1H), 7.52 (t, *J* = 5.8 Hz, 1H), 6.18 (s, 1H), 4.34 (d, *J* = 5.7 Hz, 2H), 2.39 (s, 3H).

LCMS (APCI): calcd for $C_{12}H_{11}F_3N_4O_2H^+$ ([M+H]) 301.1, found 301.1.

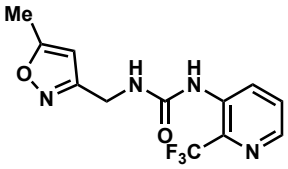

S2

Prepared according to General Minisci Functionalization with Baran Diversinates™ Procedure.

^{1}H NMR (600 MHz, DMSO-d$_6$): δ 8.42 (d, *J* = 8.5 Hz, 1H), 8.36 (d, *J* = 4.5 Hz, 1H), 8.20 (s, 1H), 7.65 (dd, *J* = 8.5, 4.5 Hz, 1H), 7.60 (t, *J* = 5.8 Hz, 1H), 6.17 (s, 1H), 4.33 (d, *J* = 5.7 Hz, 2H), 2.39 (s, 3H).

LCMS (APCI): calcd for $C_{12}H_{11}F_3N_4O_2H^+$ ([M+H]) 301.1, found 301.1.

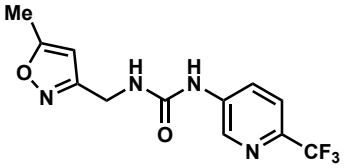

S3

Prepared according to General Minisci Functionalization with Baran Diversinates™ Procedure.

^{1}H NMR (600 MHz, DMSO-d$_6$): δ 9.37 (s, 1H), 8.69 (d, *J* = 2.5 Hz, 1H), 8.17 (dd, *J* = 8.5, 2.5 Hz, 1H), 7.77 (d, *J* = 8.7 Hz, 1H), 7.00 (t, *J* = 5.9 Hz, 1H), 6.17 (s, 1H), 4.33 (d, *J* = 5.8 Hz, 2H), 2.38 (s, 3H).

LCMS (APCI): calcd for $C_{12}H_{11}F_3N_4O_2H^+$ ([M+H]) 301.1, found 301.1.

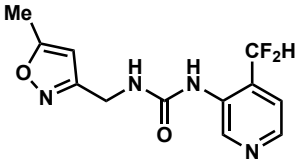

S4

Prepared according to General Minisci Functionalization with Baran Diversinates™ Procedure.

^{1}H NMR (600 MHz, DMSO-d_6): δ 8.96 (s, 1H), 8.43 (s, 1H), 8.41 (d, *J* = 5.0 Hz, 1H), 7.50 (d, *J* = 5.0 Hz, 1H), 7.26 (t, *J* = 5.9 Hz, 1H), 7.12 (t, *J* = 54.4 Hz, 1H), 6.18 (s, 1H), 4.33 (d, *J* = 5.8 Hz, 2H), 2.39 (s, 3H).

LCMS (APCI): calcd for $C_{12}H_{12}F_2N_4O_2H^+$ ([M+H]) 283.1, found 283.1.

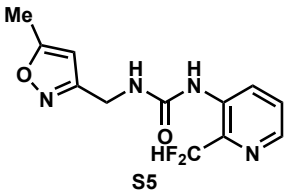

S5

Prepared according to General Minisci Functionalization with Baran Diversinates™ Procedure.

^{1}H NMR (600 MHz, DMSO-d_6): δ 8.33 (s, 1H), 8.32 – 8.29 (m, 2H), 7.51 (dd, *J* = 8.5, 4.6 Hz, 1H), 7.48 (t, *J* = 5.7 Hz, 1H), 7.00 (t, *J* = 53.8 Hz, 1H), 6.17 (s, 1H), 4.32 (d, *J* = 5.7 Hz, 2H), 2.39 (s, 3H).

LCMS (APCI): calcd for $C_{12}H_{12}F_2N_4O_2H^+$ ([M+H]) 283.1, found 283.1.

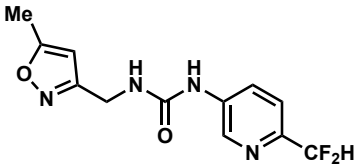

S6

Prepared according to General Minisci Functionalization with Baran Diversinates™ Procedure.

^{1}H NMR (600 MHz, DMSO-d_6): δ 9.19 (s, 1H), 8.64 (d, *J* = 2.5 Hz, 1H), 8.08 (dd, *J* = 8.7, 2.5 Hz, 1H), 7.58 (d, *J* = 8.6 Hz, 1H), 6.93 (t, *J* = 5.8 Hz, 1H), 6.85 (t, *J* = 55.3 Hz, 1H), 6.16 (s, 1H), 4.32 (d, *J* = 5.7 Hz, 2H), 2.38 (s, 3H).

LCMS (APCI): calcd for $C_{12}H_{12}F_2N_4O_2H^+$ ([M+H]) 283.1, found 283.1.

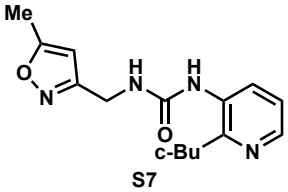

S7

Prepared according to General Minisci Functionalization with Molander BF_3K Salts Procedure.

^{1}H NMR (600 MHz, DMSO-d_6): δ 8.19 (d, *J* = 4.3 Hz, 1H), 8.12 (d, *J* = 8.2 Hz, 1H), 7.80 (s, 1H), 7.19 (t, *J* = 5.8 Hz, 1H), 7.16 (dd, *J* = 8.2, 4.8 Hz, 1H), 6.17 (s, 1H), 4.31 (d, *J* = 5.7 Hz,

2H), 3.76 (p, *J* = 8.5 Hz, 1H), 2.39 (s, 3H), 2.35 – 2.24 (m, 4H), 2.04 – 1.94 (m, 1H), 1.85 – 1.78 (m, 1H).

LCMS (APCI): calcd for $C_{15}H_{16}N_4O_2H^+$ ([M+H]) 287.2, found 287.2.

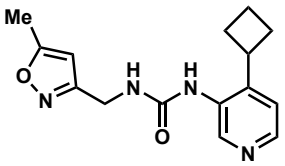

S8

Prepared according to General Minisci Functionalization with Molander BF_3K Salts Procedure.

^{1}H NMR (600 MHz, DMSO-d$_6$): δ 8.82 (s, 1H), 8.24 (s, 1H), 7.81 (s, 1H), 7.31 (s, 1H), 7.14 (t, *J* = 6.2 Hz, 1H), 6.17 (s, 1H), 4.31 (d, *J* = 5.8 Hz, 2H), 3.61 (p, *J* = 9.0, 8.5 Hz, 1H), 2.39 (s, 3H), 2.39 – 2.32 (m, 2H), 2.09 – 1.96 (m, 3H), 1.84 – 1.77 (m, 1H).

LCMS (APCI): calcd for $C_{15}H_{16}N_4O_2H^+$ ([M+H]) 287.2, found 287.2.

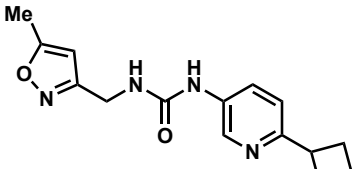

S9

Prepared according to General Minisci Functionalization with Molander BF_3K Salts Procedure.

^{1}H NMR (600 MHz, DMSO-d$_6$): δ 8.81 (s, 1H), 8.49 (s, 1H), 7.83 (d, *J* = 8.5 Hz, 1H), 7.16 (s, 1H), 6.76 (s, 1H), 6.15 (s, 1H), 4.30 (d, *J* = 5.9 Hz, 2H), 3.57 (p, *J* = 8.4, 7.9 Hz, 1H), 2.37 (s, 3H), 2.27 – 2.19 (m, 4H), 2.00 – 1.93 (m, 1H), 1.86 – 1.78 (m, 1H).

LCMS (APCI): calcd for $C_{15}H_{16}N_4O_2H^+$ ([M+H]) 287.2, found 287.2.

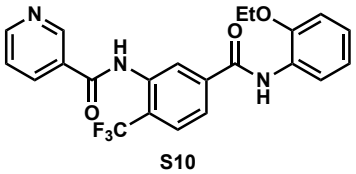

S10

Prepared according to General Minisci Functionalization with Baran Diversinates™ Procedure.

^{1}H NMR (600 MHz, DMSO-d$_6$): δ 10.57 (s, 1H), 9.76 (s, 1H), 9.13 (d, *J* = 2.3 Hz, 1H), 8.81 (dd, *J* = 4.9, 1.7 Hz, 1H), 8.31 (dt, *J* = 8.0, 2.0 Hz, 1H), 8.13 (s, 1H), 8.12 (d, *J* = 8.9 Hz, 1H), 8.01 (d, *J* = 8.2 Hz, 1H), 7.69 (d, *J* = 7.9 Hz, 1H), 7.62 (dd, *J* = 8.1, 4.6 Hz, 1H), 7.21 (t, *J* = 7.4 Hz, 1H), 7.11 (d, *J* = 8.4 Hz, 1H), 6.98 (t, *J* = 7.6 Hz, 1H), 4.11 (q, *J* = 7.0 Hz, 2H), 1.34 (t, *J* = 6.8 Hz, 3H).

LCMS (APCI): calcd for $C_{22}H_{18}F_3N_3O_3H^+$ ([M+H]) 430.1, found 430.1.

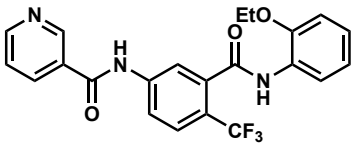

S11

Prepared according to General Minisci Functionalization with Baran Diversinates™ Procedure.

^{1}H NMR (600 MHz, DMSO-d_6): δ 10.90 (s, 1H), 9.64 (s, 1H), 9.15 (s, 1H), 8.81 (d, *J* = 4.8 Hz, 1H), 8.34 (dt, *J* = 8.1, 2.1 Hz, 1H), 8.13 (d, *J* = 2.2 Hz, 1H), 8.10 (d, *J* = 8.7 Hz, 1H), 7.85 (d, *J* = 8.7 Hz, 1H), 7.79 (d, *J* = 7.9 Hz, 1H), 7.62 (dd, *J* = 8.0, 4.7 Hz, 1H), 7.18 (t, *J* = 7.9 Hz, 1H), 7.09 (d, *J* = 8.2 Hz, 1H), 6.97 (t, *J* = 7.6 Hz, 1H), 4.09 (q, *J* = 6.9 Hz, 2H), 1.35 (t, *J* = 7.0 Hz, 3H).

LCMS (APCI): calcd for $C_{22}H_{18}F_3N_3O_3H^+$ ([M+H]) 430.1, found 430.1.

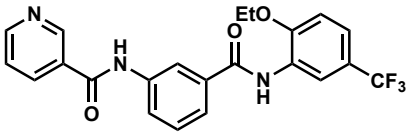

S12

Prepared according to General Minisci Functionalization with Baran Diversinates™ Procedure.

^{1}H NMR (600 MHz, DMSO-d_6): δ 10.68 (s, 1H), 9.55 (s, 1H), 9.15 (d, *J* = 2.3 Hz, 1H), 8.79 (dd, *J* = 4.7, 1.7 Hz, 1H), 8.41 (s, 1H), 8.34 (dt, *J* = 8.0, 2.0 Hz, 1H), 8.28 (d, *J* = 2.4 Hz, 1H), 8.01 (dd, *J* = 8.0, 2.2 Hz, 1H), 7.73 (d, *J* = 7.7 Hz, 1H), 7.60 (dd, *J* = 8.0, 4.8 Hz, 1H), 7.57 (t, *J* = 8.1 Hz, 1H), 7.54 (dd, *J* = 8.8, 2.8 Hz, 1H), 7.30 (d, *J* = 8.6 Hz, 1H), 4.24 (q, *J* = 7.0 Hz, 2H), 1.42 (t, *J* = 7.0 Hz, 3H).

LCMS (APCI): calcd for $C_{22}H_{18}F_3N_3O_3H^+$ ([M+H]) 430.1, found 430.1.

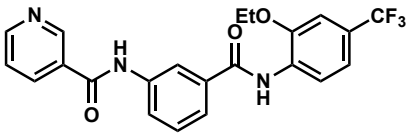

S13

Prepared according to General Minisci Functionalization with Baran Diversinates™ Procedure.

^{1}H NMR (600 MHz, DMSO-d_6): δ 10.68 (s, 1H), 9.52 (s, 1H), 9.15 (s, 1H), 8.79 (d, *J* = 4.9 Hz, 1H), 8.42 (s, 1H), 8.34 (dt, *J* = 8.1, 2.0 Hz, 1H), 8.19 (d, *J* = 8.2 Hz, 1H), 8.03 (dd, *J* = 8.0, 2.2 Hz, 1H), 7.73 (d, *J* = 7.7 Hz, 1H), 7.60 (dd, *J* = 8.0, 4.9 Hz, 1H), 7.57 (t, *J* = 7.9 Hz, 1H), 7.39 (s, 1H), 7.37 (d, *J* = 9.1 Hz, 1H), 4.24 (q, *J* = 6.9 Hz, 2H), 1.42 (t, *J* = 6.9 Hz, 3H).

LCMS (APCI): calcd for $C_{22}H_{18}F_3N_3O_3H^+$ ([M+H]) 430.1, found 430.1.

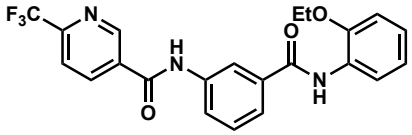

S14

Prepared according to General Minisci Functionalization with Baran Diversinates™ Procedure.

^{1}H NMR (600 MHz, DMSO-d$_6$): δ 10.85 (s, 1H), 9.35 (s, 1H), 9.28 (s, 1H), 8.61 (d, *J* = 8.0 Hz, 1H), 8.37 (s, 1H), 8.13 (d, *J* = 8.1 Hz, 1H), 8.01 (d, *J* = 7.8 Hz, 1H), 7.87 (d, *J* = 7.9 Hz, 1H), 7.74 (d, *J* = 8.0 Hz, 1H), 7.57 (t, *J* = 7.9 Hz, 1H), 7.16 (t, *J* = 8.1 Hz, 1H), 7.10 (d, *J* = 8.2 Hz, 1H), 6.97 (t, *J* = 7.7 Hz, 1H), 4.12 (q, *J* = 7.0 Hz, 2H), 1.38 (t, *J* = 6.7 Hz, 3H).

LCMS (APCI): calcd for $C_{22}H_{18}F_3N_3O_3H^+$ ([M+H]) 430.1, found 430.1

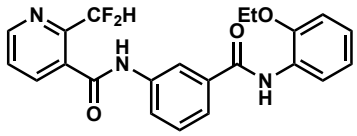

S15

Prepared according to General Minisci Functionalization with Baran Diversinates™ Procedure.

^{1}H NMR (600 MHz, DMSO-d$_6$): δ 10.87 (s, 1H), 9.33 (s, 1H), 8.85 (d, *J* = 4.7 Hz, 1H), 8.35 (s, 1H), 8.23 (d, *J* = 7.8 Hz, 1H), 7.92 – 7.87 (m, 2H), 7.75 (dd, *J* = 7.9, 5.0 Hz, 1H), 7.73 (d, *J* = 7.8 Hz, 1H), 7.55 (t, *J* = 7.9 Hz, 1H), 7.22 (t, *J* = 53.9 Hz, 1H), 7.16 (t, *J* = 7.8 Hz, 1H), 7.10 (d, *J* = 8.2 Hz, 1H), 6.98 (t, *J* = 7.6 Hz, 1H), 4.13 (q, *J* = 6.9 Hz, 2H), 1.39 (t, *J* = 6.9 Hz, 3H).

LCMS (APCI): calcd for $C_{22}H_{19}F_2N_3O_3H^+$ ([M+H]) 412.2, found 412.1.

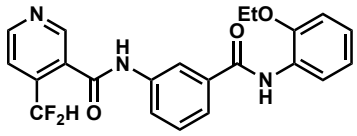

S16

Prepared according to General Minisci Functionalization with Baran Diversinates™ Procedure.

^{1}H NMR (600 MHz, DMSO-d$_6$): δ 10.96 (s, 1H), 9.33 (s, 1H), 9.06 (s, 1H), 8.94 (d, *J* = 5.1 Hz, 1H), 8.37 (s, 1H), 7.93 – 7.88 (m, 2H), 7.78 (d, *J* = 5.1 Hz, 1H), 7.74 (d, *J* = 7.7 Hz, 1H), 7.56 (t, *J* = 7.9 Hz, 1H), 7.42 (t, *J* = 54.6 Hz, 1H), 7.16 (t, *J* = 7.8 Hz, 1H), 7.11 (d, *J* = 8.1 Hz, 1H), 6.98 (t, *J* = 7.6 Hz, 1H), 4.13 (q, *J* = 7.0 Hz, 2H), 1.39 (t, *J* = 6.9 Hz, 3H).

LCMS (APCI): calcd for $C_{22}H_{19}F_2N_3O_3H^+$ ([M+H]) 412.2, found 412.1.

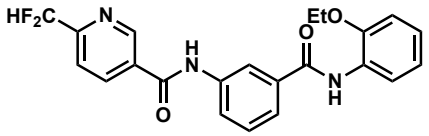

S17

Prepared according to General Minisci Functionalization with Baran Diversinates™ Procedure.

^{1}H NMR (600 MHz, DMSO-d_6): δ 10.78 (s, 1H), 9.35 (s, 1H), 9.23 (s, 1H), 8.53 (dd, *J* = 8.1, 2.3 Hz, 1H), 8.38 (s, 1H), 8.02 (d, *J* = 8.0 Hz, 1H), 7.91 (d, *J* = 8.1 Hz, 1H), 7.88 (d, *J* = 7.9 Hz, 1H), 7.74 (d, *J* = 7.7 Hz, 1H), 7.57 (t, *J* = 7.9 Hz, 1H), 7.16 (d, *J* = 7.7 Hz, 1H), 7.11 (d, *J* = 8.3 Hz, 1H), 7.09 (t, *J* = 55.1 Hz, 1H), 6.98 (d, *J* = 7.6 Hz, 1H), 4.13 (q, *J* = 6.9 Hz, 2H), 1.39 (t, *J* = 6.9 Hz, 3H).

LCMS (APCI): calcd for $C_{22}H_{19}F_2N_3O_3H^+$ ([M+H]) 412.2, found 412.1.

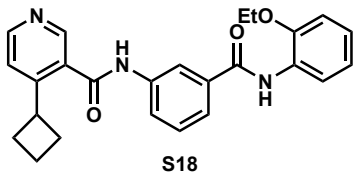

S18

Prepared according to General Minisci Functionalization with Molander BF_3K Salts Procedure.

^{1}H NMR (600 MHz, DMSO-d_6): δ 10.75 (s, 1H), 9.31 (s, 1H), 8.80 – 8.64 (m, 2H), 8.36 (s, 1H), 7.91 (d, *J* = 7.9 Hz, 1H), 7.87 (dd, *J* = 8.0, 2.2 Hz, 1H), 7.71 (d, *J* = 7.7 Hz, 1H), 7.59 (d, *J* = 5.1 Hz, 1H), 7.54 (t, *J* = 7.9 Hz, 1H), 7.16 (td, *J* = 7.8, 1.7 Hz, 1H), 7.10 (d, *J* = 8.0 Hz, 1H), 6.98 (t, *J* = 7.5 Hz, 1H), 4.13 (q, *J* = 6.9 Hz, 2H), 3.92 (p, *J* = 8.8 Hz, 1H), 2.34 – 2.25 (m, 2H), 2.22 – 2.11 (m, 2H), 2.05 – 1.93 (m, 1H), 1.84 – 1.75 (m, 1H), 1.39 (t, *J* = 7.0 Hz, 3H).

LCMS (APCI): calcd for $C_{25}H_{25}N_3O_3H^+$ ([M+H]) 416.2, found 416.2.

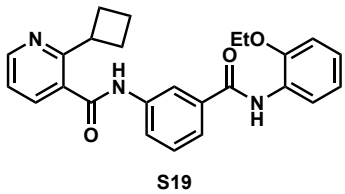

S19

Prepared according to General Minisci Functionalization with Molander BF_3K Salts Procedure.

^{1}H NMR (600 MHz, DMSO-d_6): δ 10.66 (s, 1H), 9.31 (s, 1H), 8.70 (dd, *J* = 5.0, 1.7 Hz, 1H), 8.37 (s, 1H), 7.93 – 7.88 (m, 2H), 7.87 (d, *J* = 7.8 Hz, 1H), 7.70 (d, *J* = 7.7 Hz, 1H), 7.53 (t, *J* = 7.9 Hz, 1H), 7.40 (dd, *J* = 7.7, 4.9 Hz, 1H), 7.16 (t, *J* = 7.2 Hz, 1H), 7.10 (d, *J* = 8.1 Hz, 1H), 6.98 (t, *J* = 7.6 Hz, 1H), 4.13 (q, *J* = 6.9 Hz, 2H), 3.98 (p, *J* = 8.6 Hz, 1H), 2.45 – 2.34 (m, 2H), 2.26 – 2.16 (m, 2H), 2.03 – 1.91 (m, 1H), 1.84 – 1.75 (m, 1H), 1.39 (t, *J* = 6.9 Hz, 3H).

LCMS (APCI): calcd for $C_{25}H_{25}N_3O_3H^+$ ([M+H]) 416.2, found 416.2.

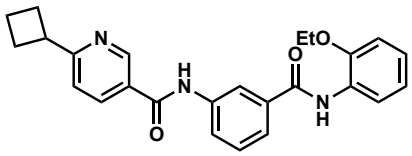

S20

Prepared according to General Minisci Functionalization with Molander BF_3K Salts Procedure.

^{1}H NMR (600 MHz, DMSO-d_6): δ 10.62 (s, 1H), 9.33 (s, 1H), 9.12 (d, *J* = 2.3 Hz, 1H), 8.40 – 8.32 (m, 2H), 8.01 (dd, *J* = 8.1, 2.2 Hz, 1H), 7.89 (dd, *J* = 7.9, 1.6 Hz, 1H), 7.72 (d, *J* = 7.7 Hz, 1H), 7.60 – 7.50 (m, 2H), 7.16 (td, *J* = 7.8, 1.7 Hz, 1H), 7.10 (d, *J* = 8.1 Hz, 1H), 6.98 (t, *J* = 7.5 Hz, 1H), 4.13 (q, *J* = 6.9 Hz, 2H), 3.79 (p, *J* = 8.6 Hz, 1H), 2.41 – 2.28 (m, 4H), 2.11 – 2.00 (m, 1H), 1.94 – 1.85 (m, 1H), 1.39 (t, *J* = 7.0 Hz, 3H).

LCMS (APCI): calcd for $C_{25}H_{25}N_3O_3H^+$ ([M+H]) 416.2, found 416.2.

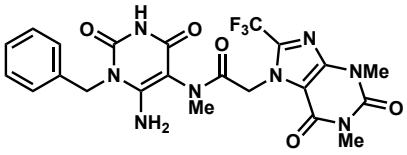

S21

Prepared according to General Minisci Functionalization with Baran Diversinates™ Procedure.

^{1}H NMR (600 MHz, DMSO-d_6): δ 11.01 (s, 1H), 7.35 (t, *J* = 7.5 Hz, 2H), 7.30 – 7.21 (m, 5H), 5.16 (q, *J* = 17.5, 17.0 Hz, 2H), 5.05 (d, *J* = 16.5 Hz, 1H), 4.96 (d, *J* = 16.6 Hz, 1H), 3.46 (s, 3H), 3.23 (s, 3H), 2.92 (s, 3H).

LCMS (APCI): calcd for $C_{22}H_{21}F_3N_8O_5H^+$ ([M+H]) 535.2, found 535.2.

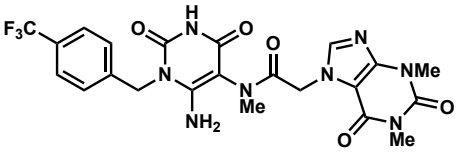

S22

Prepared according to General Minisci Functionalization with Baran Diversinates™ Procedure.

^{1}H NMR (600 MHz, DMSO-d_6): δ 11.07 (s, 1H), 7.99 (s, 1H), 7.73 (d, *J* = 8.1 Hz, 2H), 7.47 (d, *J* = 8.0 Hz, 2H), 5.23 (q, *J* = 17.7 Hz, 2H), 5.08 (d, *J* = 16.6 Hz, 1H), 4.95 (d, *J* = 16.6 Hz, 1H), 3.45 (s, 3H), 3.20 (s, 3H), 2.93 (s, 3H).

LCMS (APCI): calcd for $C_{22}H_{21}F_3N_8O_5H^+$ ([M+H]) 535.2, found 535.2.

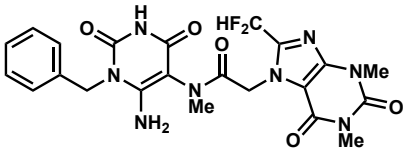

S23

Prepared according to General Minisci Functionalization with Baran Diversinates™ Procedure.

^{1}H NMR (600 MHz, DMSO-d$_6$): δ 11.04 (s, 1H), 7.35 (t, *J* = 7.5 Hz, 2H), 7.30 – 7.23 (m, 5H), 7.12 (t, *J* = 51.7 Hz, 1H), 5.25 (s, 2H), 5.15 (q, *J* = 17.0 Hz, 2H), 3.46 (s, 3H), 3.22 (s, 3H), 2.92 (s, 3H).

LCMS (APCI): calcd for $C_{22}H_{22}F_2N_8O_5H^+$ ([M+H]) 517.2, found 517.2.

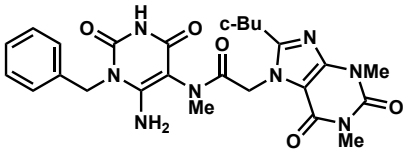

S24

Prepared according to General Minisci Functionalization with Molander BF_3K Salts Procedure.

^{1}H NMR (600 MHz, DMSO-d$_6$): δ 11.02 (s, 1H), 7.35 (t, *J* = 7.5 Hz, 2H), 7.29 – 7.23 (m, 5H), 5.16 (s, 2H), 4.97 (d, *J* = 17.2 Hz, 1H), 4.85 (d, *J* = 17.0 Hz, 1H), 3.55 (p, *J* = 8.6 Hz, 1H), 3.46 (s, 3H), 3.19 (s, 3H), 2.91 (s, 3H), 2.45 – 2.36 (m, 1H), 2.28 – 2.17 (m, 3H), 2.00 – 1.89 (m, 1H), 1.87 – 1.79 (m, 1H).

LCMS (APCI): calcd for $C_{25}H_{28}N_8O_5H^+$ ([M+H]) 521.2, found 521.2.

References:

(1) Lall, M. S.; Bassyouni, A.; Bradow, J.; Brown, M.; Bundesmann, M.; Chen, J.; Ciszewski, G.; Hagen, A. E.; Hyek, D.; Jenkinson, S.; et al. Late-Stage Lead Diversification Coupled with Quantitative Nuclear Magnetic Resonance Spectroscopy to Identify New Structure–Activity Relationship Vectors at Nanomole-Scale Synthesis: Application to Loratadine, a Human Histamine H1 Receptor Inverse Agonist. *Journal of Medicinal Chemistry* **2020**, *63* (13), 7268-7292. DOI: 10.1021/acs.jmedchem.0c00483.

(2) Seritan, S.; Bannwarth, C.; Fales, B. S.; Hohenstein, E. G.; Isborn, C. M.; Kokkila-Schumacher, S. I. L.; Li, X.; Liu, F.; Luehr, N.; Snyder Jr, J. W.; et al. TeraChem: A graphical processing unit-accelerated electronic structure package for large-scale ab initio molecular dynamics. *WIREs Computational Molecular Science* **2021**, *11* (2), e1494, https://doi.org/10.1002/wcms.1494. DOI: https://doi.org/10.1002/wcms.1494 (acccessed 2022/11/18).

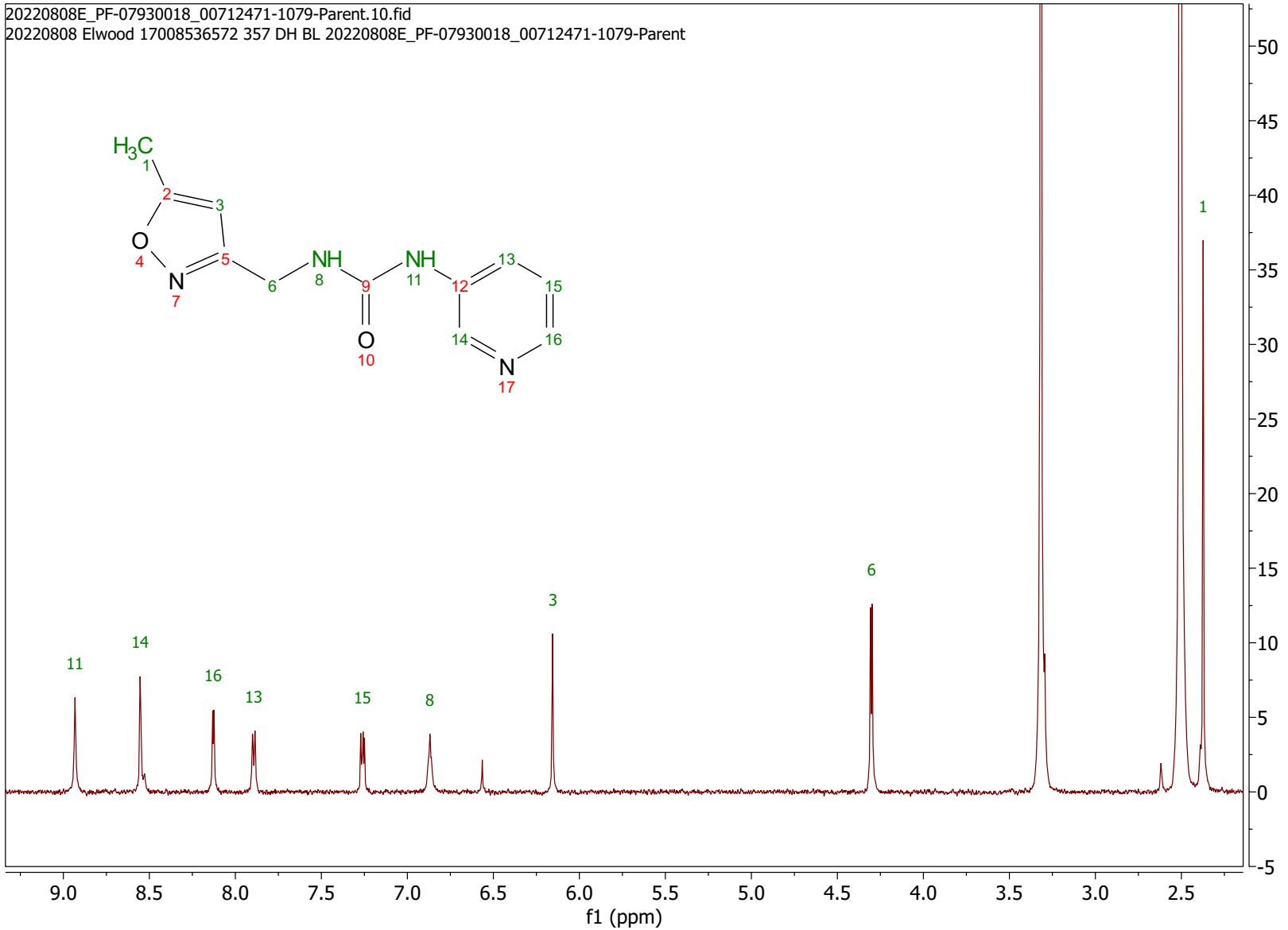
20220808E_PF-07930018_00712471-1079-Parent.10.fid
20220808 Elwood 17008536572 357 DH BL 20220808E_PF-07930018_00712471-1079-Parent
H3C
1
2
3
O
4
N
7
5
6
NH
8
9
O
10
NH
11
12
13
15
14
16
N
17
11
14
16
13
15
8
3
6
1
9.0
8.5
8.0
7.5
7.0
6.5
6.0
5.5
5.0
4.5
4.0
3.5
3.0
2.5
f1 (ppm)
50
45
40
35
30
25
20
15
10
5
0
-5

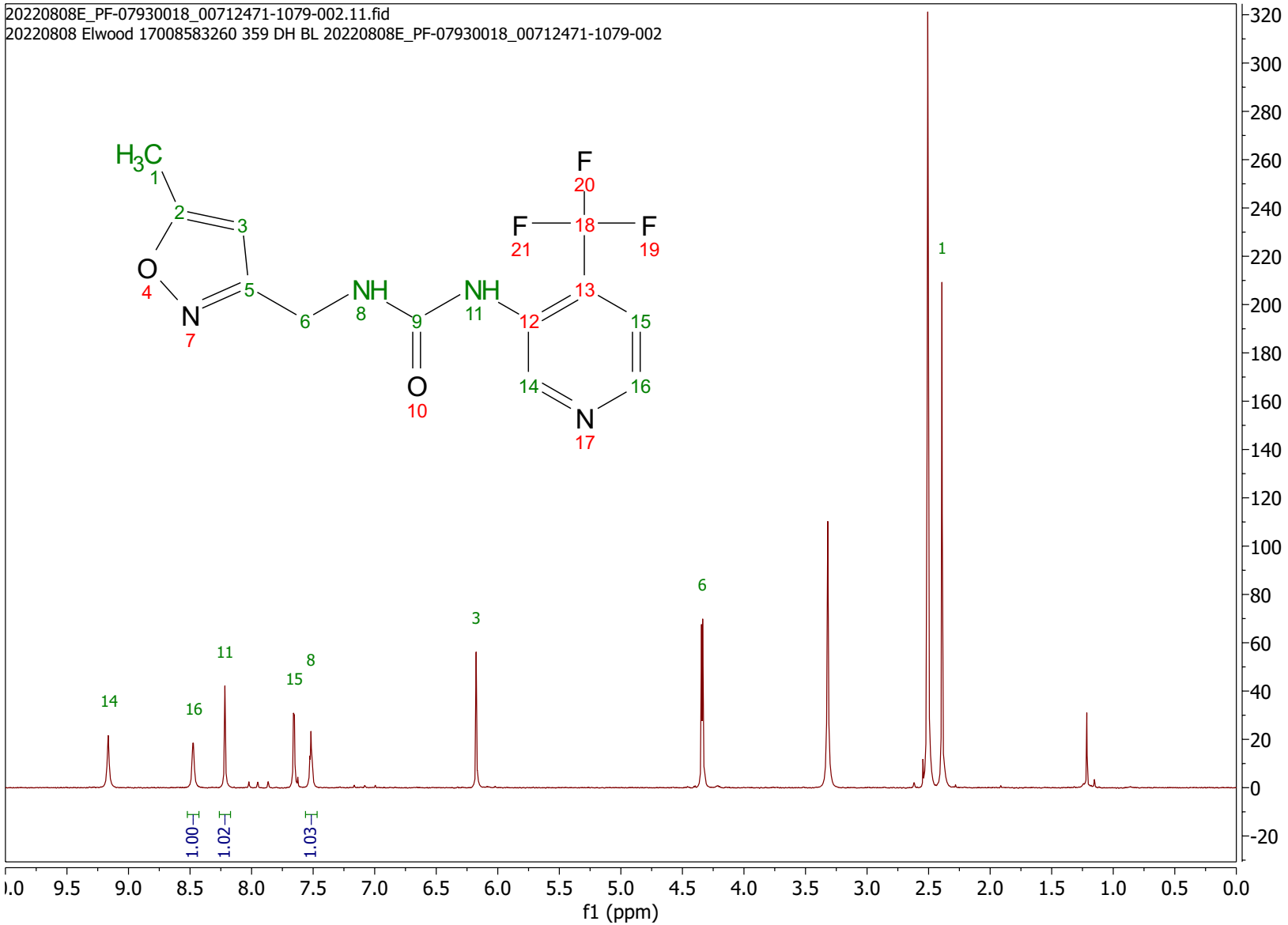
20220808E_PF-07930018_00712471-1079-002.11.fid
20220808 Elwood 17008583260 359 DH BL 20220808E_PF-07930018_00712471-1079-002
H3C
1
2
3
O
4
N
5
7
6
NH
8
9
O
10
NH
11
12
13
15
14
16
N
17
F
20
F
18
F
21
19
1
6
3
11
8
15
14
16
1.00
1.02
1.03
f1 (ppm)

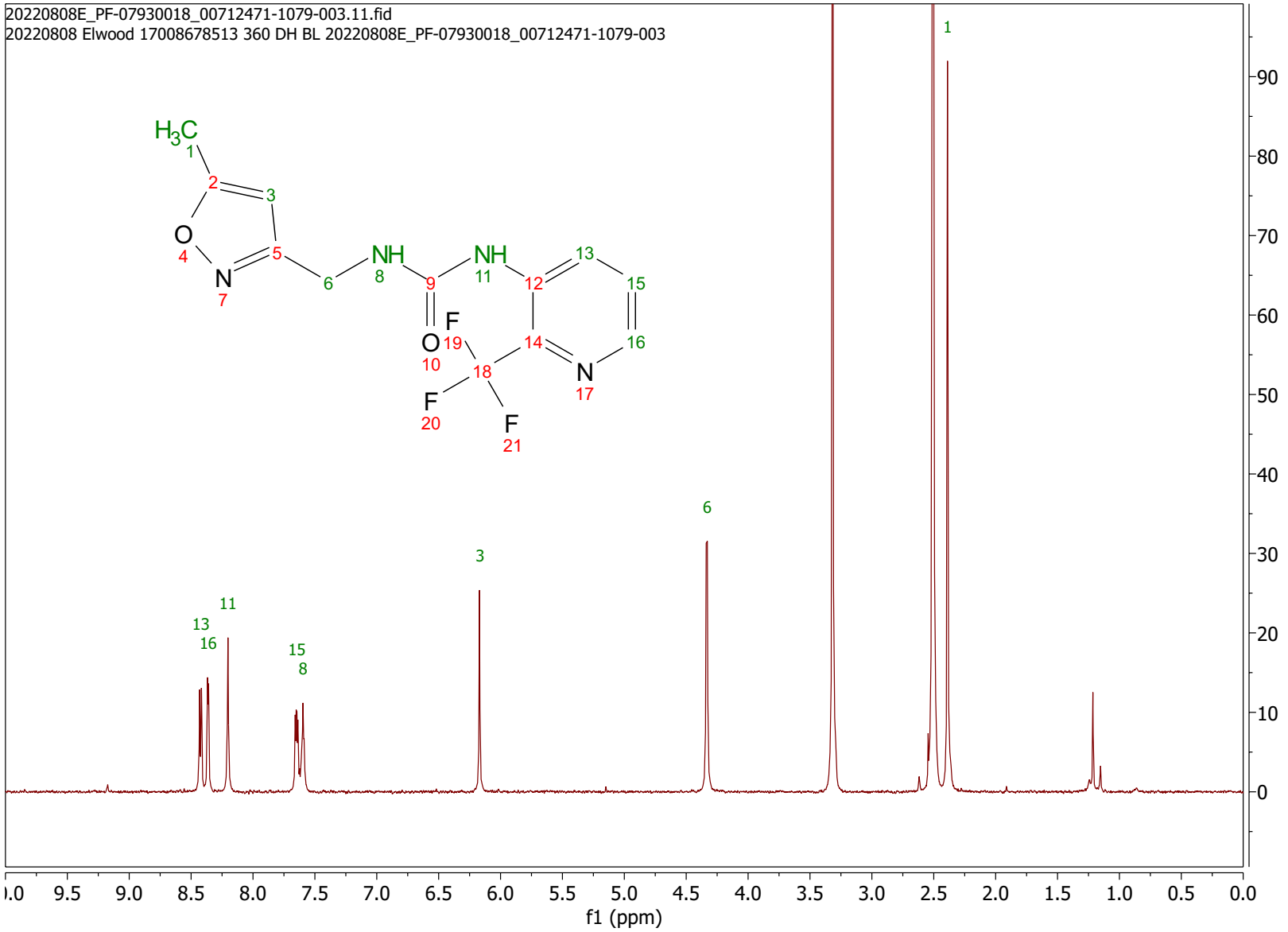
20220808E_PF-07930018_00712471-1079-003.11.fid
20220808 Elwood 17008678513 360 DH BL 20220808E_PF-07930018_00712471-1079-003
H3C
1
2
3
O
4
N
7
5
6
NH
8
9
NH
11
12
13
15
F
O
10
19
14
16
18
N
17
F
20
F
21
1
6
3
11
13
16
15
8
f1 (ppm)

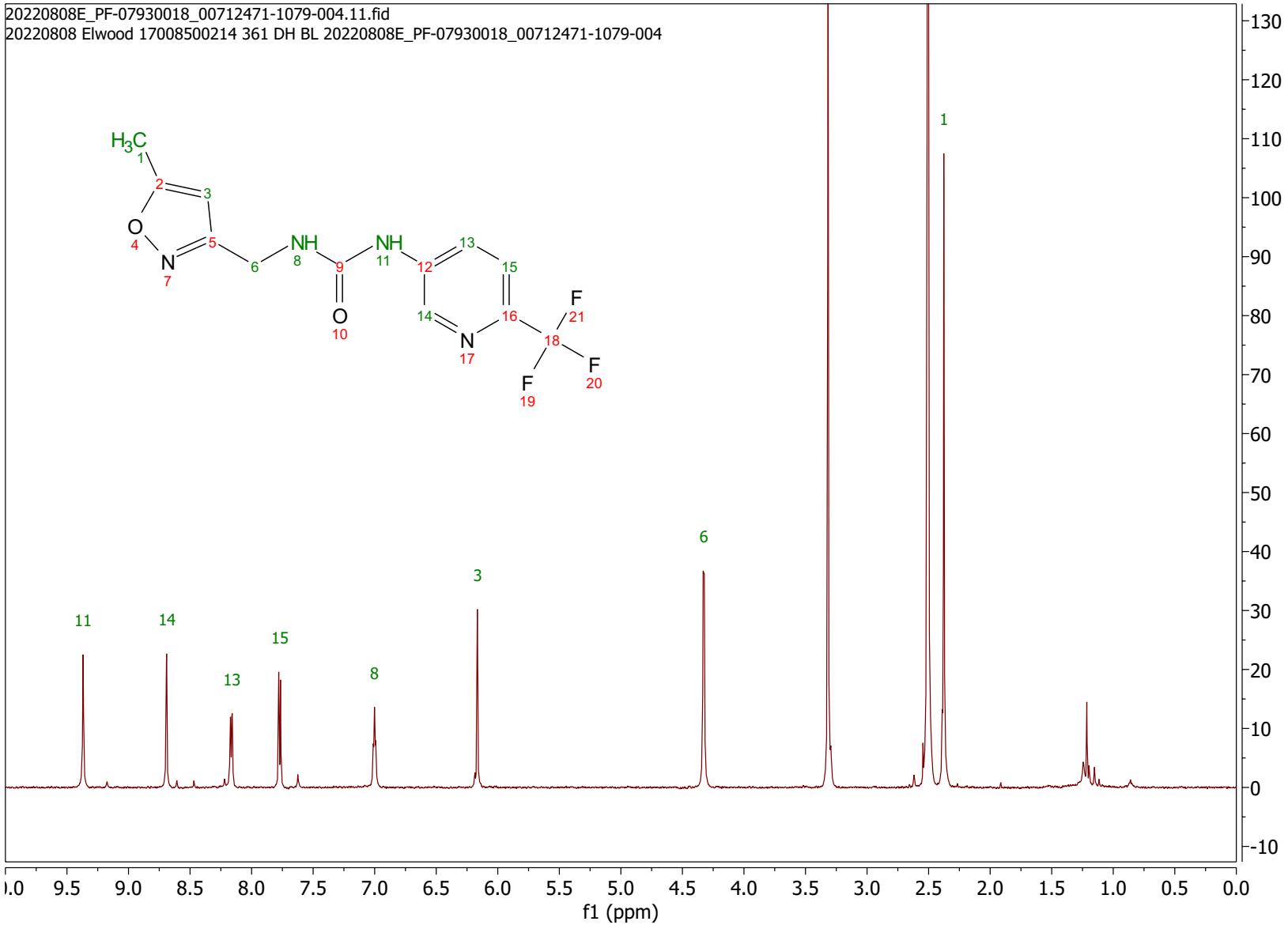
20220808E_PF-07930018_00712471-1079-004.11.fid
20220808 Elwood 17008500214 361 DH BL 20220808E_PF-07930018_00712471-1079-004
H3C
1
2
3
O
4
N
5
7
6
NH
8
9
O
10
NH
11
12
13
15
14
16
N
17
F
21
18
F
20
F
19
11
14
13
15
8
3
6
1
f1 (ppm)

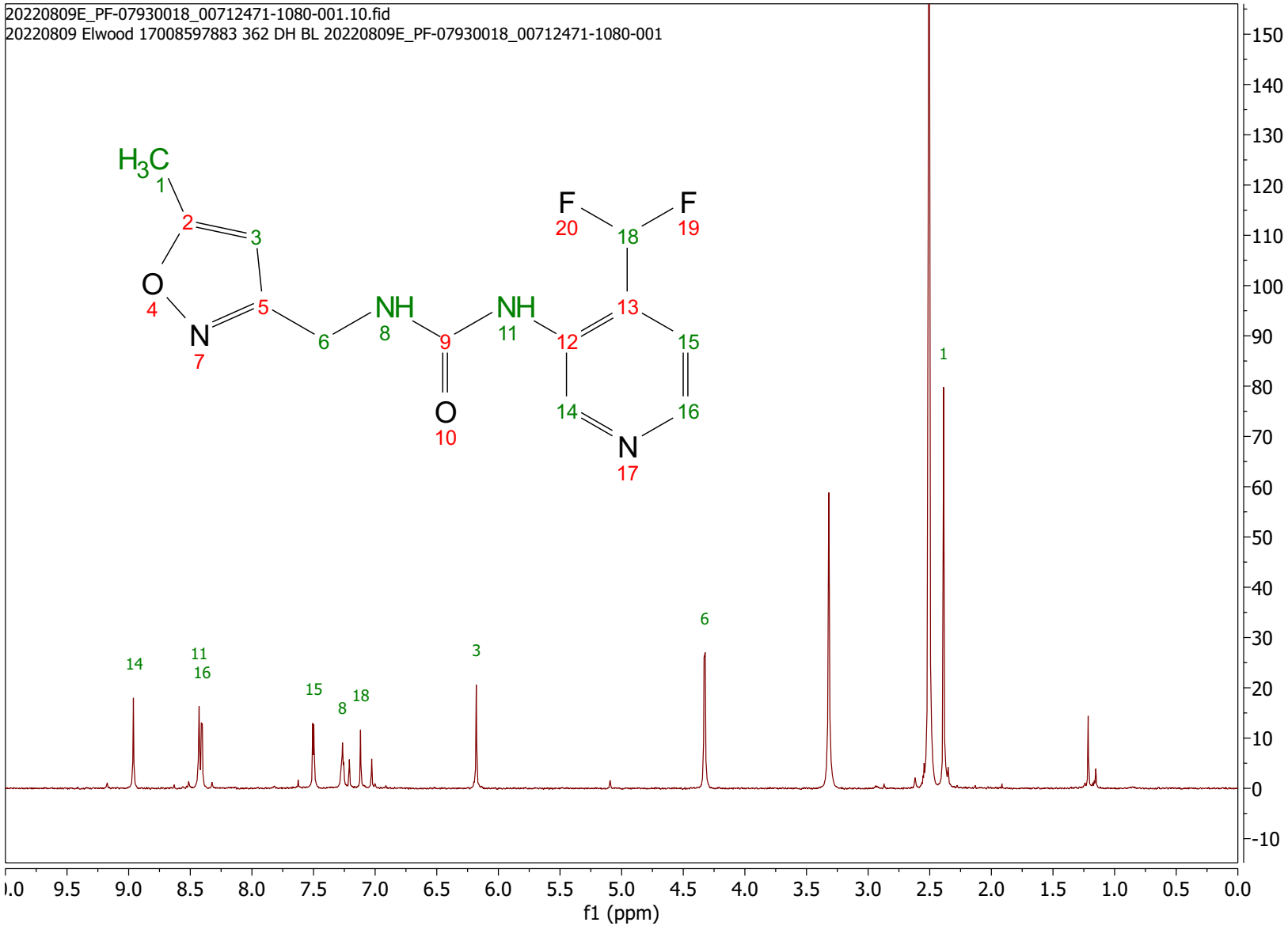
20220809E_PF-07930018_00712471-1080-001.10.fid
20220809 Elwood 17008597883 362 DH BL 20220809E_PF-07930018_00712471-1080-001
H3C
1
2
3
O
4
5
N
7
6
NH
8
9
O
10
NH
11
12
13
F
20
18
F
19
15
14
16
N
17
14
11
16
15
8
18
3
6
1
f1 (ppm)

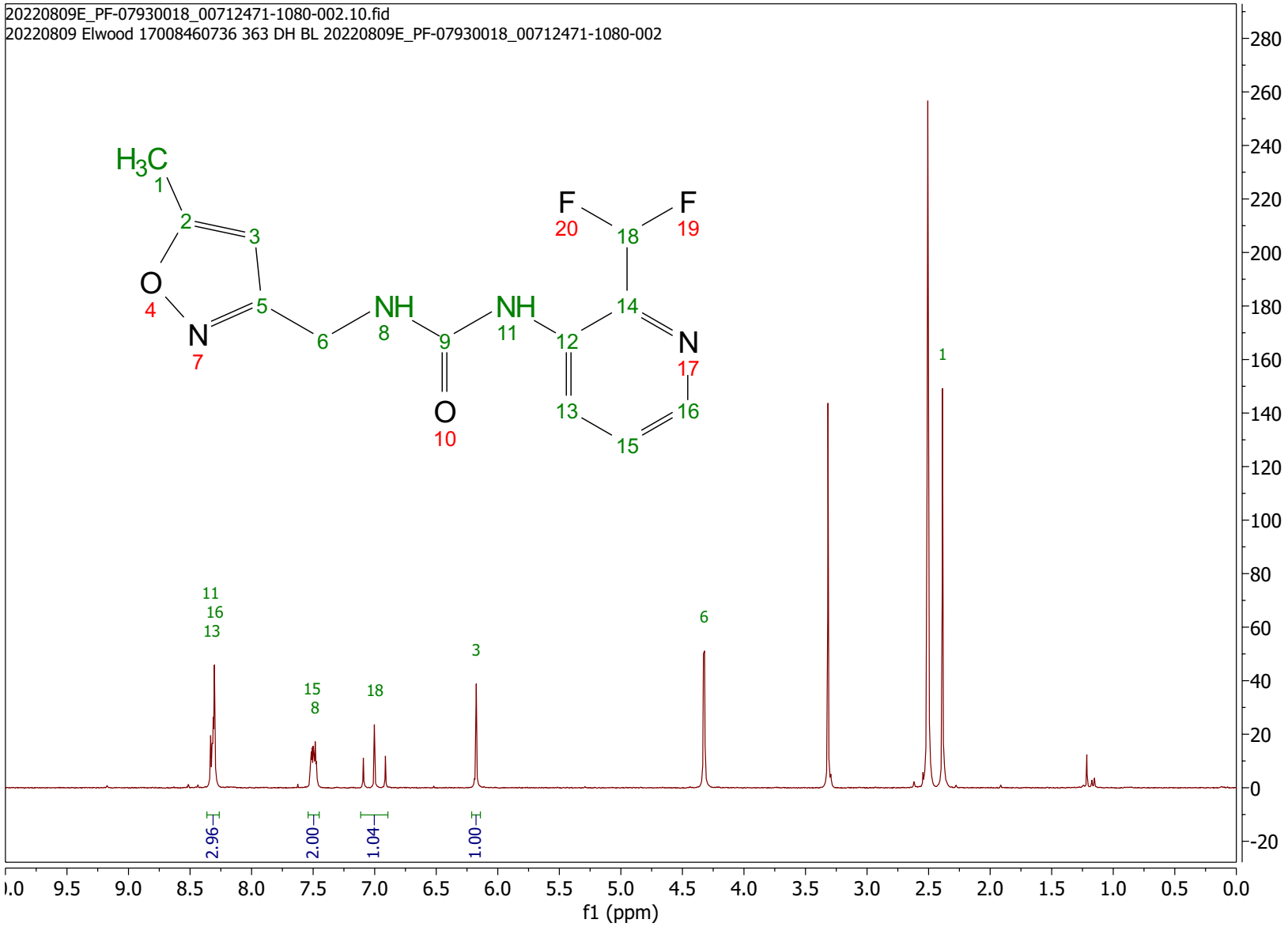
20220809E_PF-07930018_00712471-1080-002.10.fid
20220809 Elwood 17008460736 363 DH BL 20220809E_PF-07930018_00712471-1080-002
H3C
1
2
3
O
4
5
N
7
6
NH
8
9
O
10
NH
11
12
F
20
18
F
19
14
N
17
13
16
15
11
16
13
15
8
18
3
6
1
2.96
2.00
1.04
1.00
f1 (ppm)

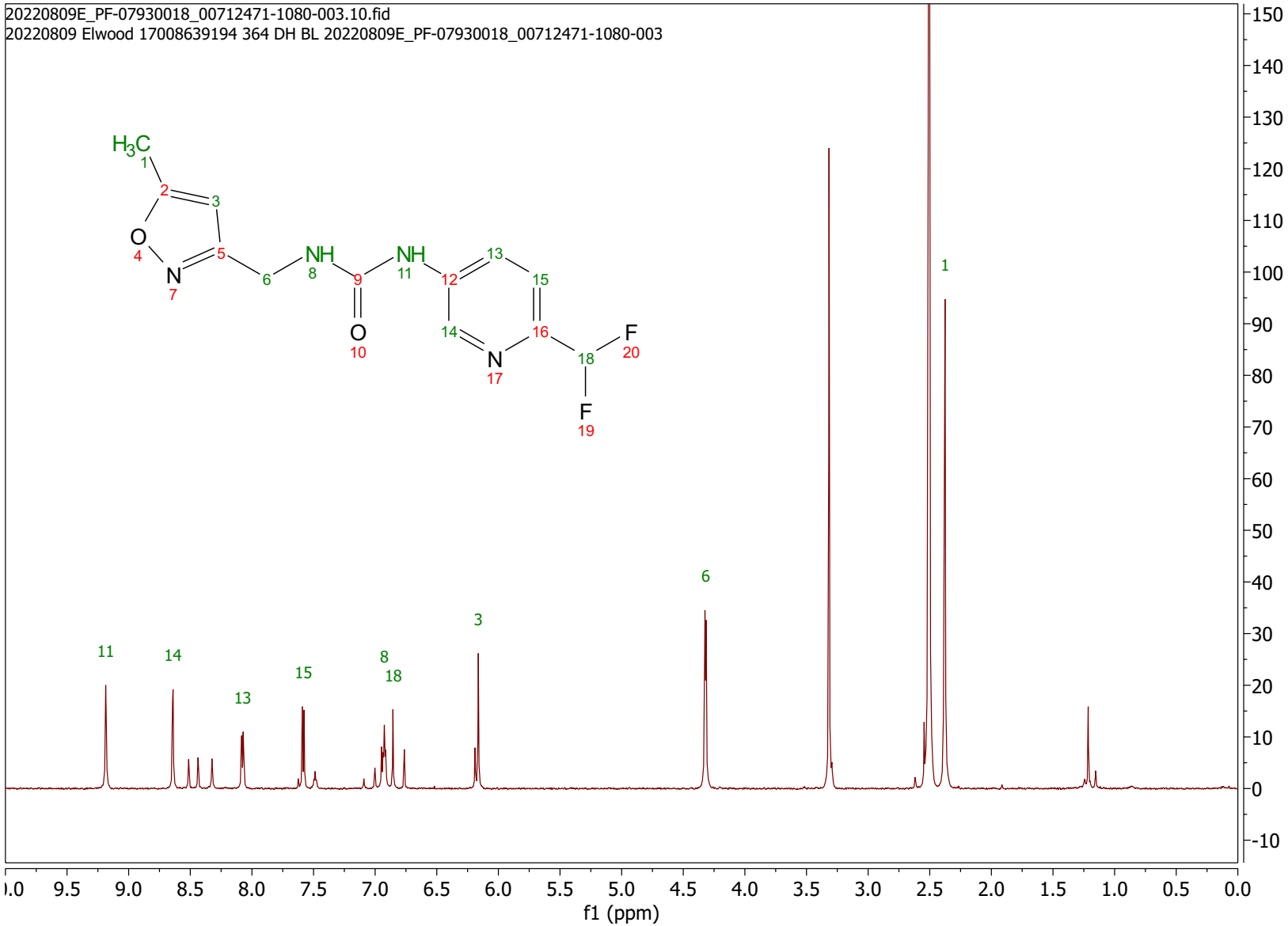
20220809E_PF-07930018_00712471-1080-003.10.fid
20220809 Elwood 17008639194 364 DH BL 20220809E_PF-07930018_00712471-1080-003
H3C
1
2
3
O
4
N
7
5
6
NH
8
9
O
10
NH
11
12
13
14
15
16
N
17
18
F
20
F
19
11
14
13
15
8
18
3
6
1
f1 (ppm)

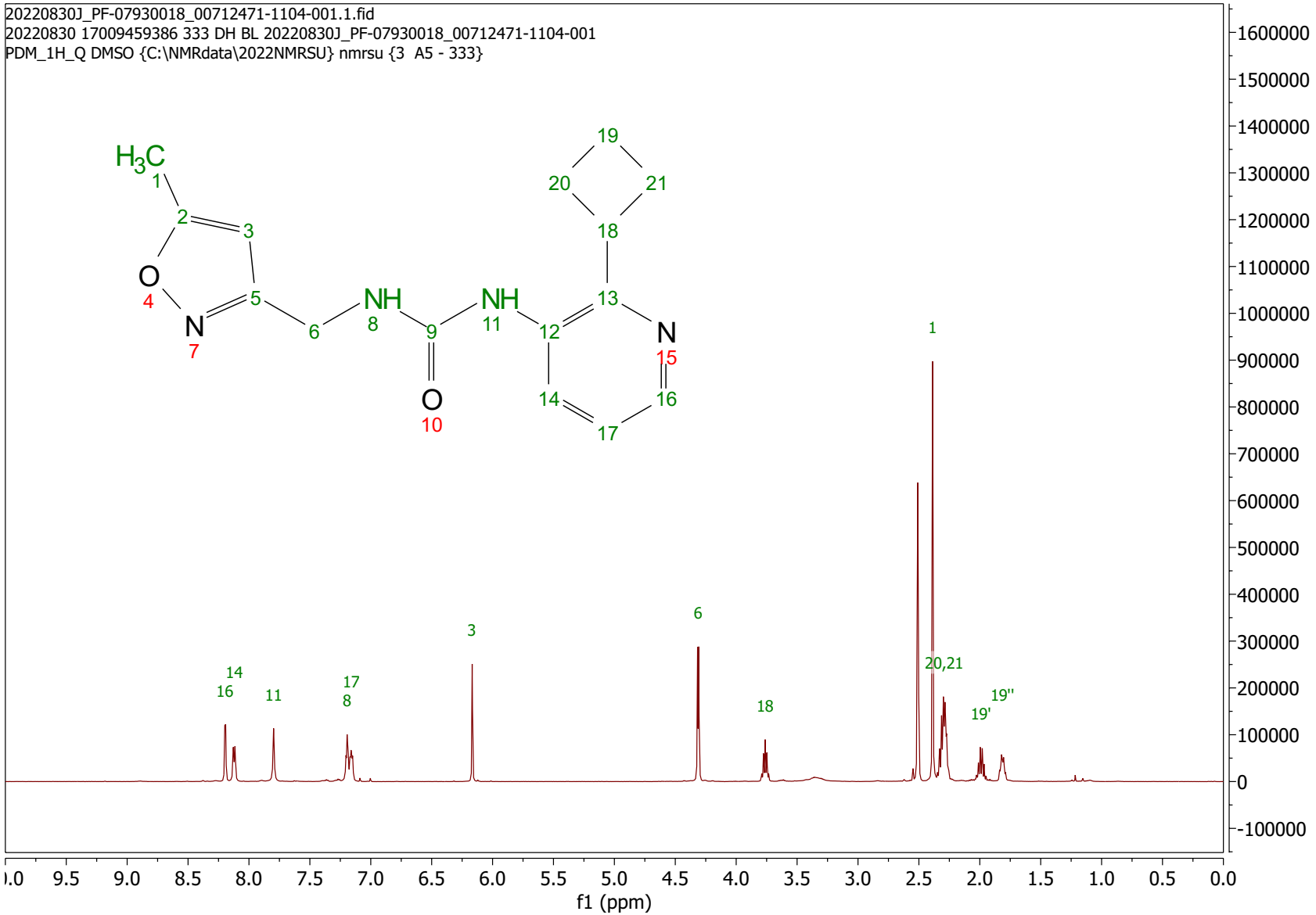
20220830J_PF-07930018_00712471-1104-001.1.fid
20220830 17009459386 333 DH BL 20220830J_PF-07930018_00712471-1104-001
PDM_1H_Q DMSO {C:\NMRdata\2022NMRSU} nmrsu {3 A5 - 333}
H3C
O
N
NH
NH
O
N
1
2
3
4
5
6
7
8
9
10
11
12
13
14
15
16
17
18
19
20
21
1
6
3
14
16
11
17
8
18
20,21
19'
19''
f1 (ppm)

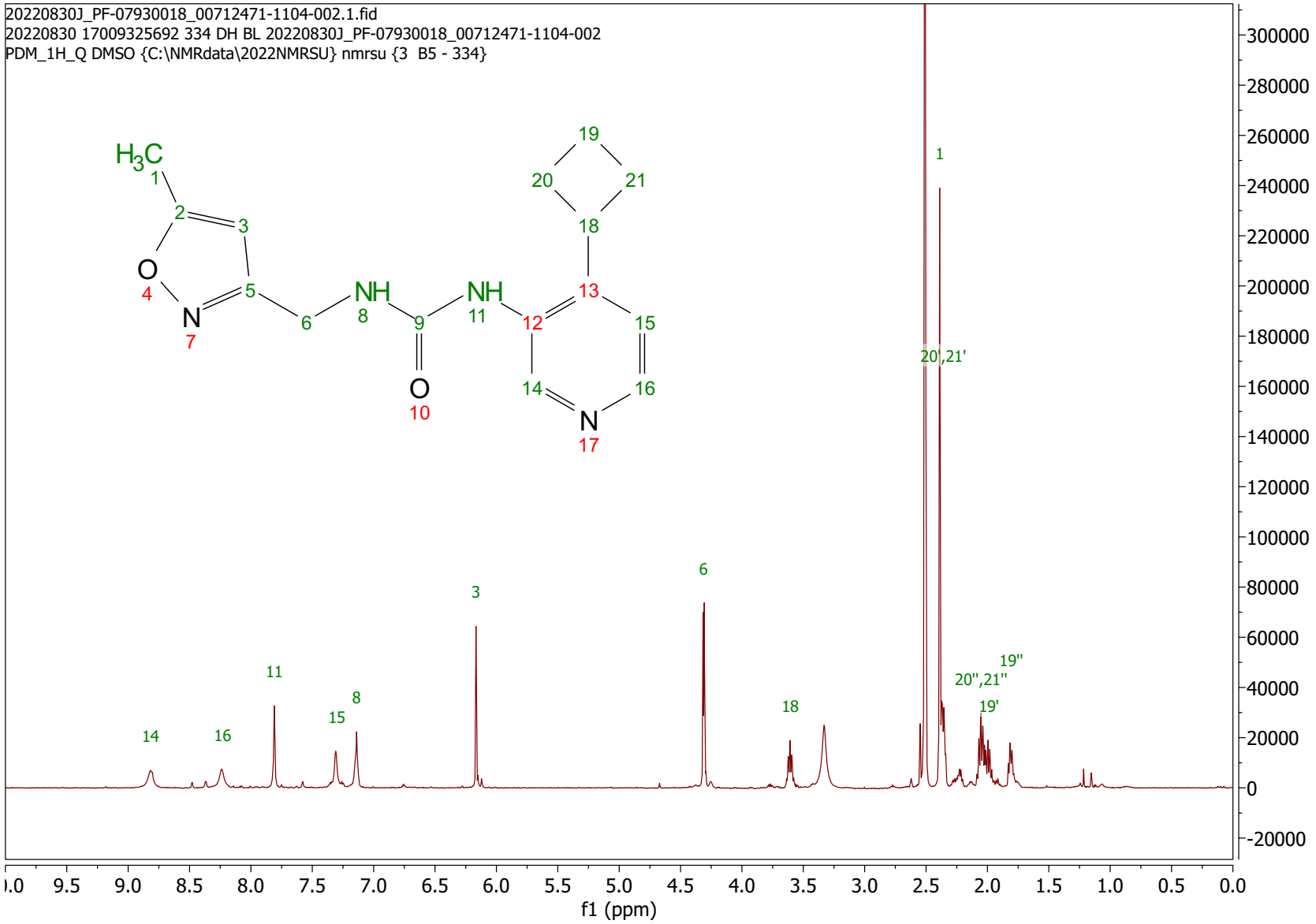
20220830J_PF-07930018_00712471-1104-002.1.fid
20220830 17009325692 334 DH BL 20220830J_PF-07930018_00712471-1104-002
PDM_1H_Q DMSO {C:\NMRdata\2022NMRSU} nmrsu {3 B5 - 334}
H3C
O
N
NH
NH
f1 (ppm)

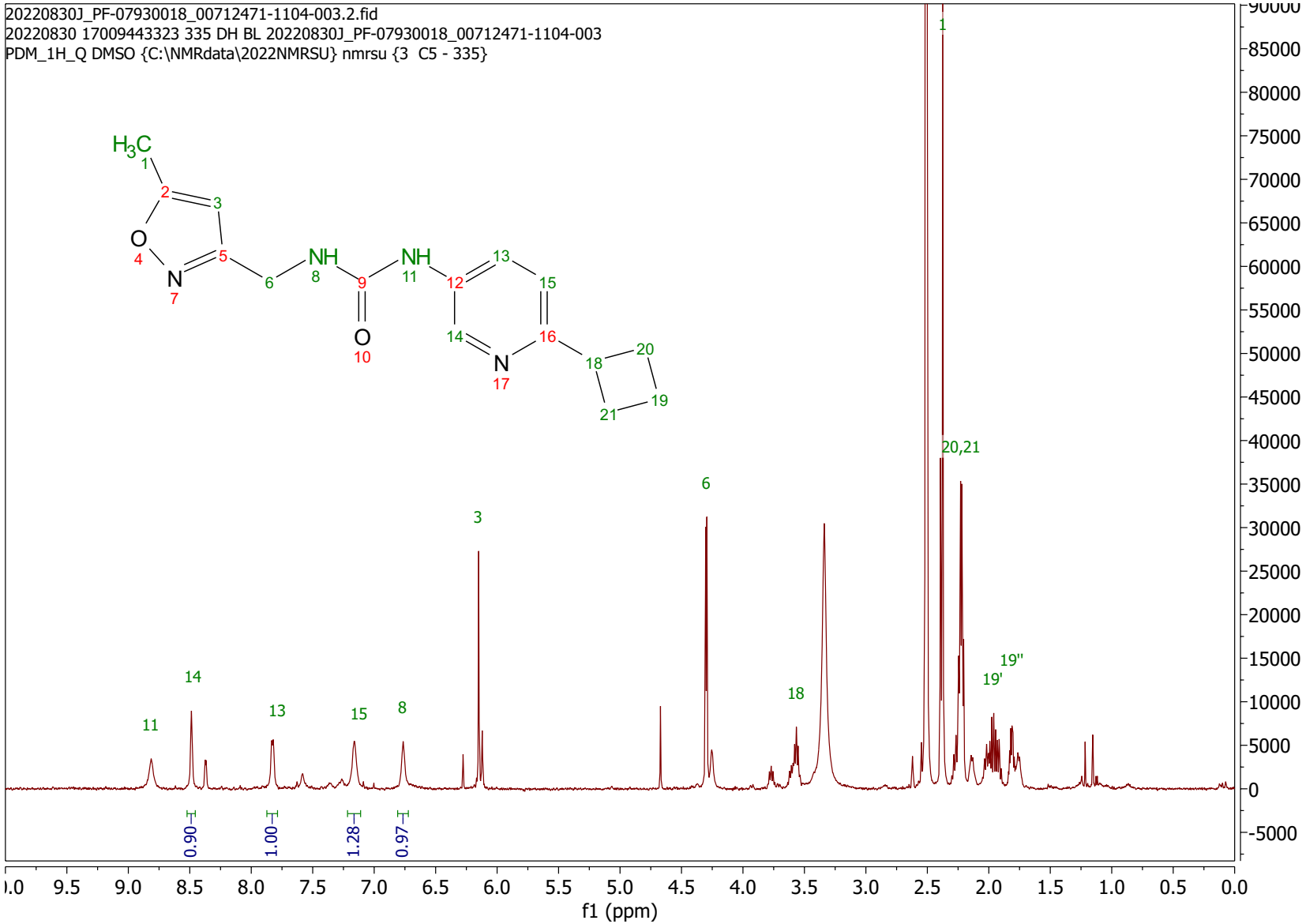
20220830J_PF-07930018_00712471-1104-003.2.fid
20220830 17009443323 335 DH BL 20220830J_PF-07930018_00712471-1104-003
PDM_1H_Q DMSO {C:\NMRdata\2022NMRSU} nmrsu {3 C5 - 335}
H3C
O
N
NH
NH
O
N
1
2
3
4
5
6
7
8
9
10
11
12
13
14
15
16
17
18
19
20
21
1
20,21
6
3
18
14
11
13
15
8
19'
19''
0.90
1.00
1.28
0.97
f1 (ppm)

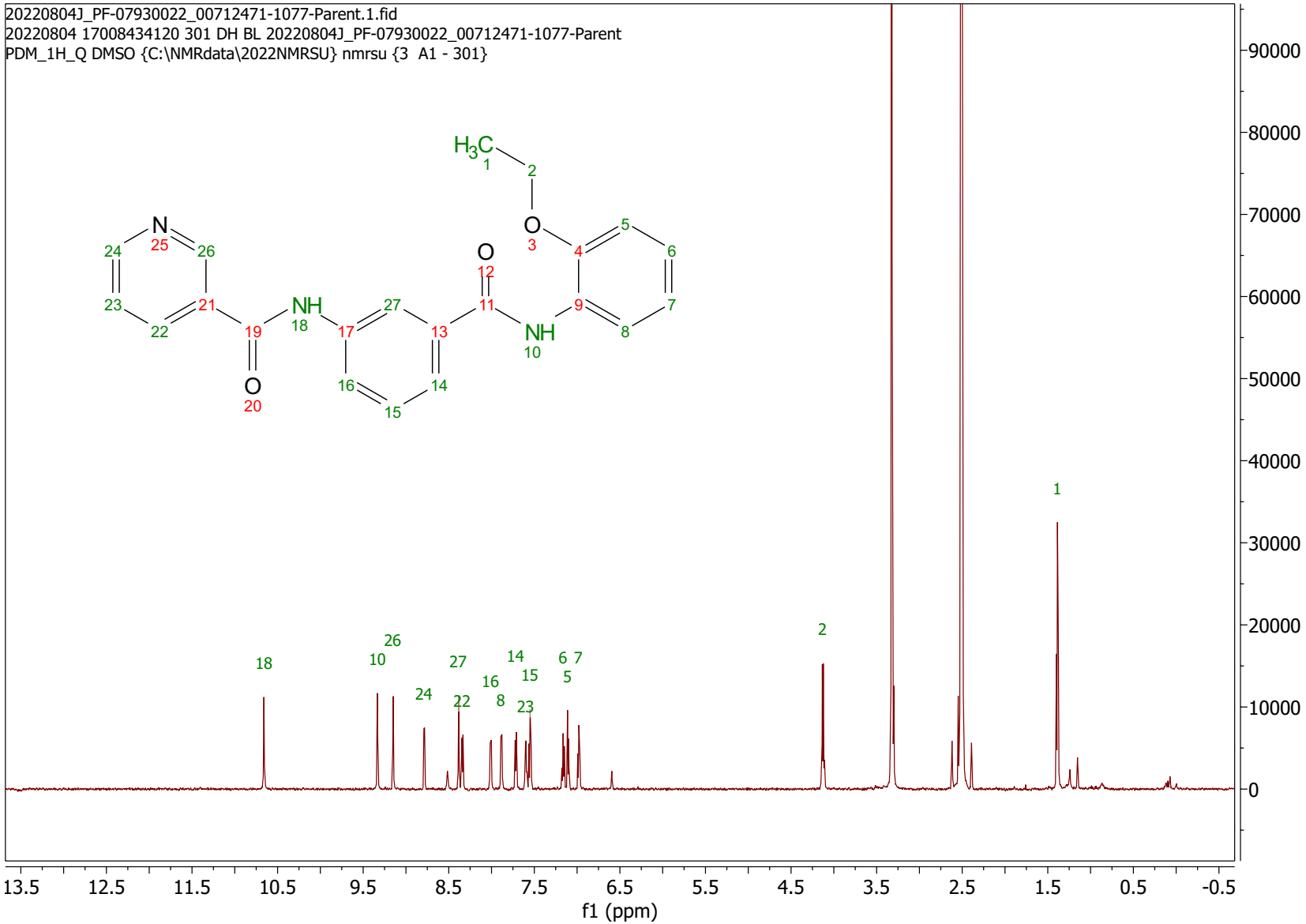
20220804J_PF-07930022_00712471-1077-Parent.1.fid
20220804 17008434120 301 DH BL 20220804J_PF-07930022_00712471-1077-Parent
PDM_1H_Q DMSO {C:\NMRdata\2022NMRSU} nmrsu {3 A1 - 301}
H3C
1
2
O
3
4
5
6
7
8
9
NH
10
11
O
12
13
14
15
16
17
NH
18
19
O
20
21
22
23
24
N
25
26
27
18
10
26
24
22
27
16
8
14
15
23
6 7
5
2
1
90000
80000
70000
60000
50000
40000
30000
20000
10000
0
13.5
12.5
11.5
10.5
9.5
8.5
7.5
6.5
5.5
4.5
3.5
2.5
1.5
0.5
-0.5
f1 (ppm)

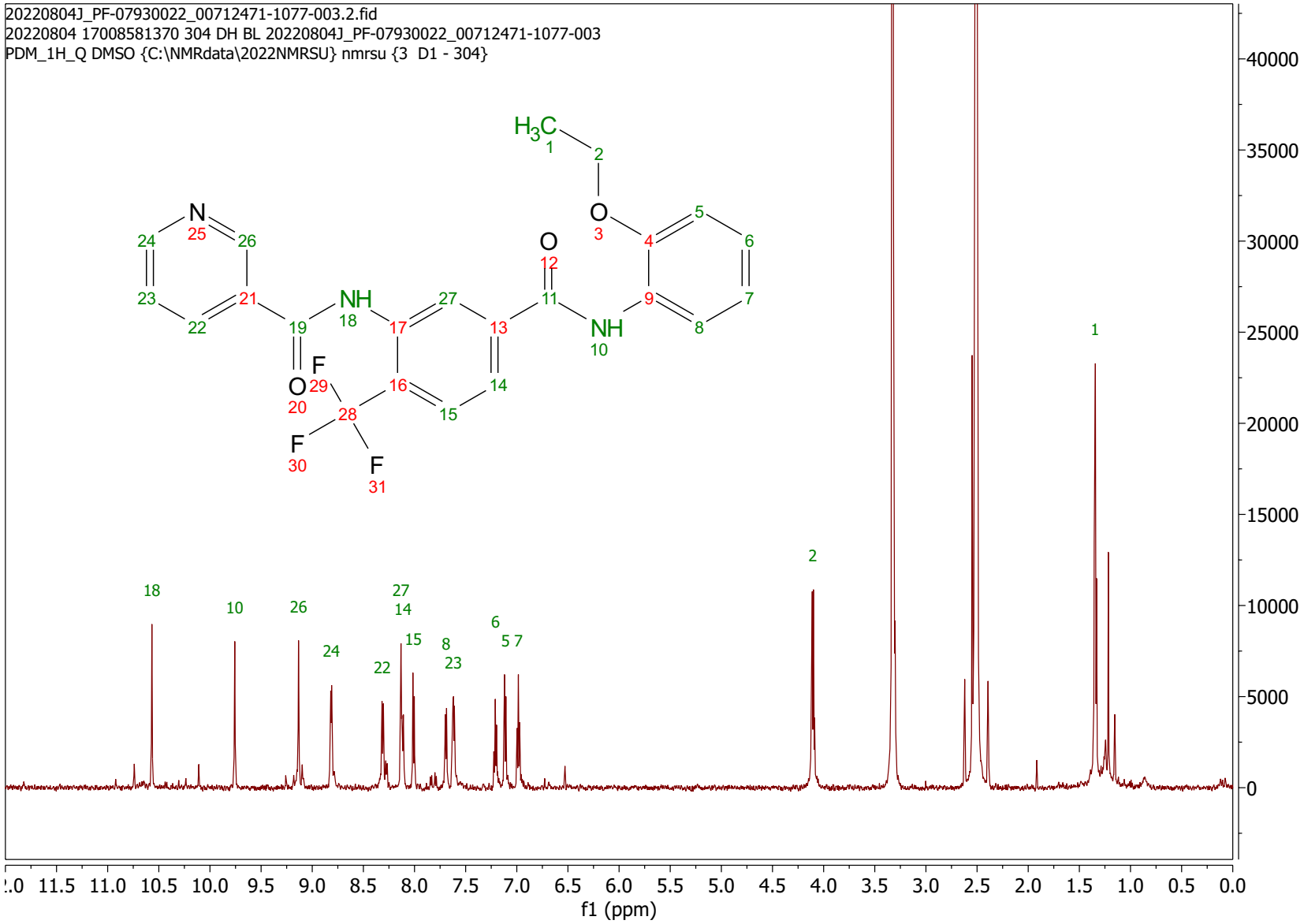
20220804J_PF-07930022_00712471-1077-003.2.fid
20220804 17008581370 304 DH BL 20220804J_PF-07930022_00712471-1077-003
PDM_1H_Q DMSO {C:\NMRdata\2022NMRSU} nmrsu {3 D1 - 304}
H3C
1
2
O
3
4
5
6
7
8
9
N
25
24
26
23
22
21
19
NH
18
17
27
13
11
O
12
NH
10
F
O
29
20
28
16
14
15
F
30
F
31
40000
35000
30000
25000
20000
15000
10000
5000
0
18
10
26
24
22
27
14
15
8
23
6
5 7
2
1
11.5 11.0 10.5 10.0 9.5 9.0 8.5 8.0 7.5 7.0 6.5 6.0 5.5 5.0 4.5 4.0 3.5 3.0 2.5 2.0 1.5 1.0 0.5 0.0
f1 (ppm)

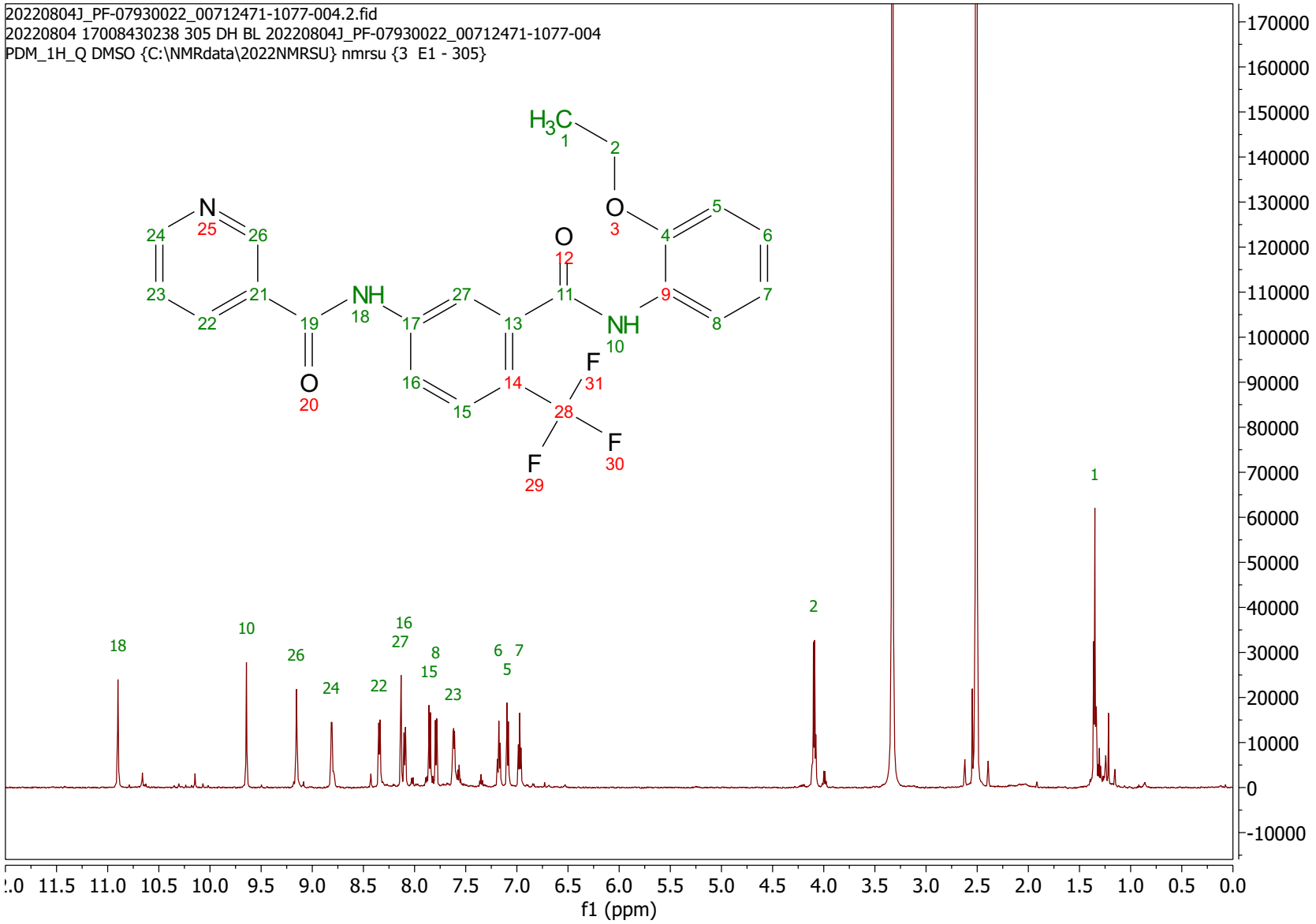
20220804J_PF-07930022_00712471-1077-004.2.fid
20220804 17008430238 305 DH BL 20220804J_PF-07930022_00712471-1077-004
PDM_1H_Q DMSO {C:\NMRdata\2022NMRSU} nmrsu {3 E1 - 305}
f1 (ppm)

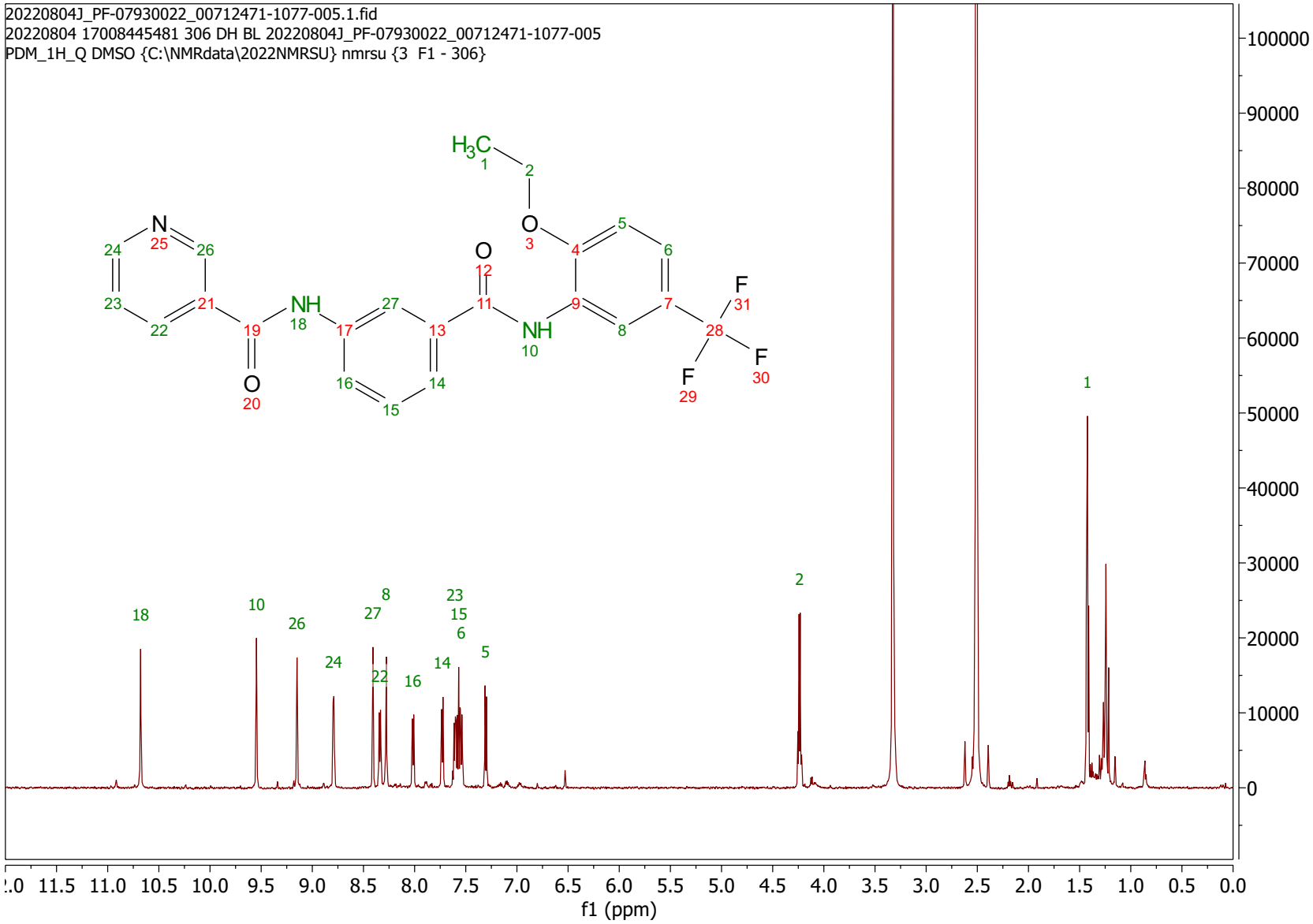
20220804J_PF-07930022_00712471-1077-005.1.fid
20220804 17008445481 306 DH BL 20220804J_PF-07930022_00712471-1077-005
PDM_1H_Q DMSO {C:\NMRdata\2022NMRSU} nmrsu {3 F1 - 306}
f1 (ppm)

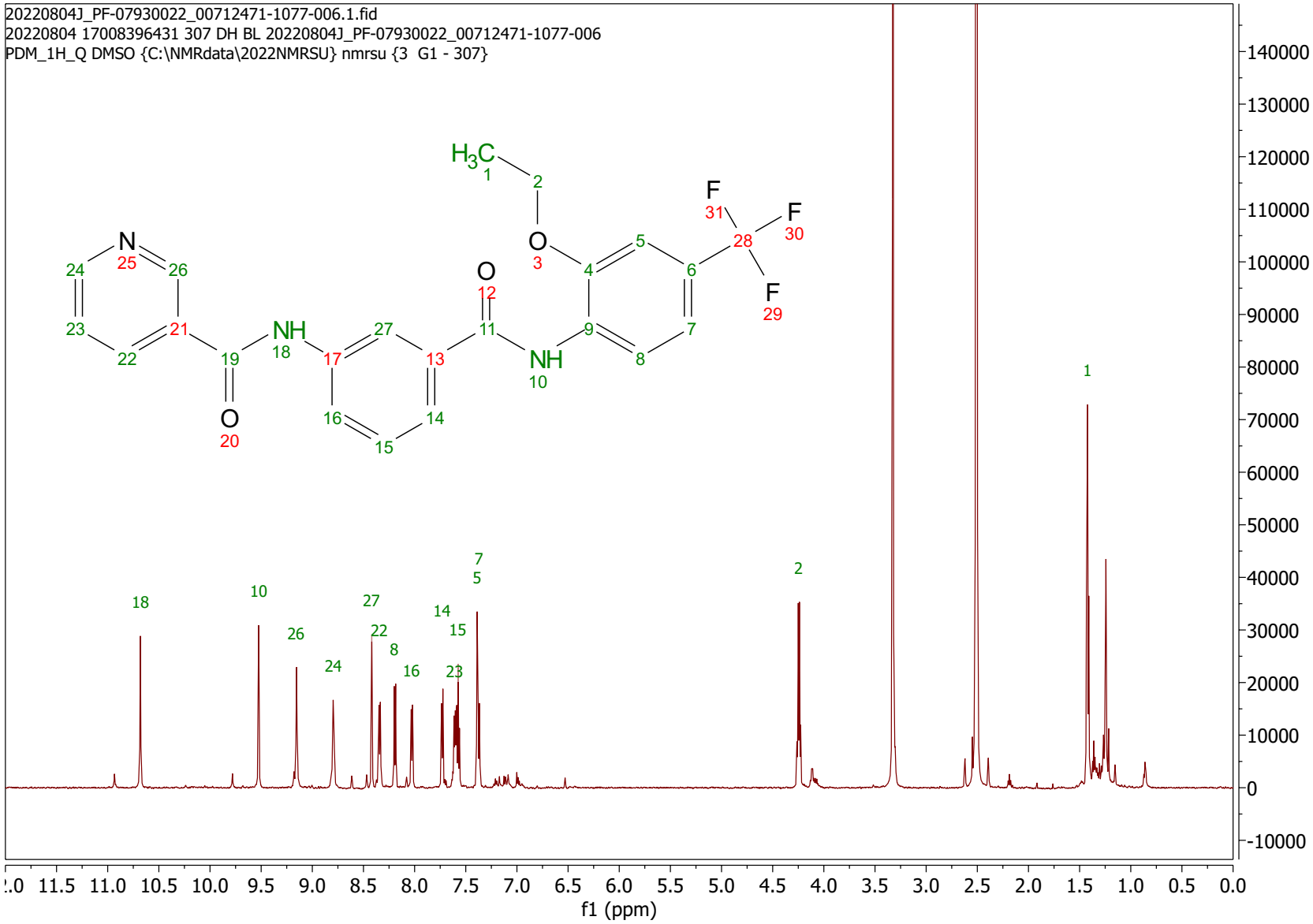
20220804J_PF-07930022_00712471-1077-006.1.fid
20220804 17008396431 307 DH BL 20220804J_PF-07930022_00712471-1077-006
PDM_1H_Q DMSO {C:\NMRdata\2022NMRSU} nmrsu {3 G1 - 307}
f1 (ppm)

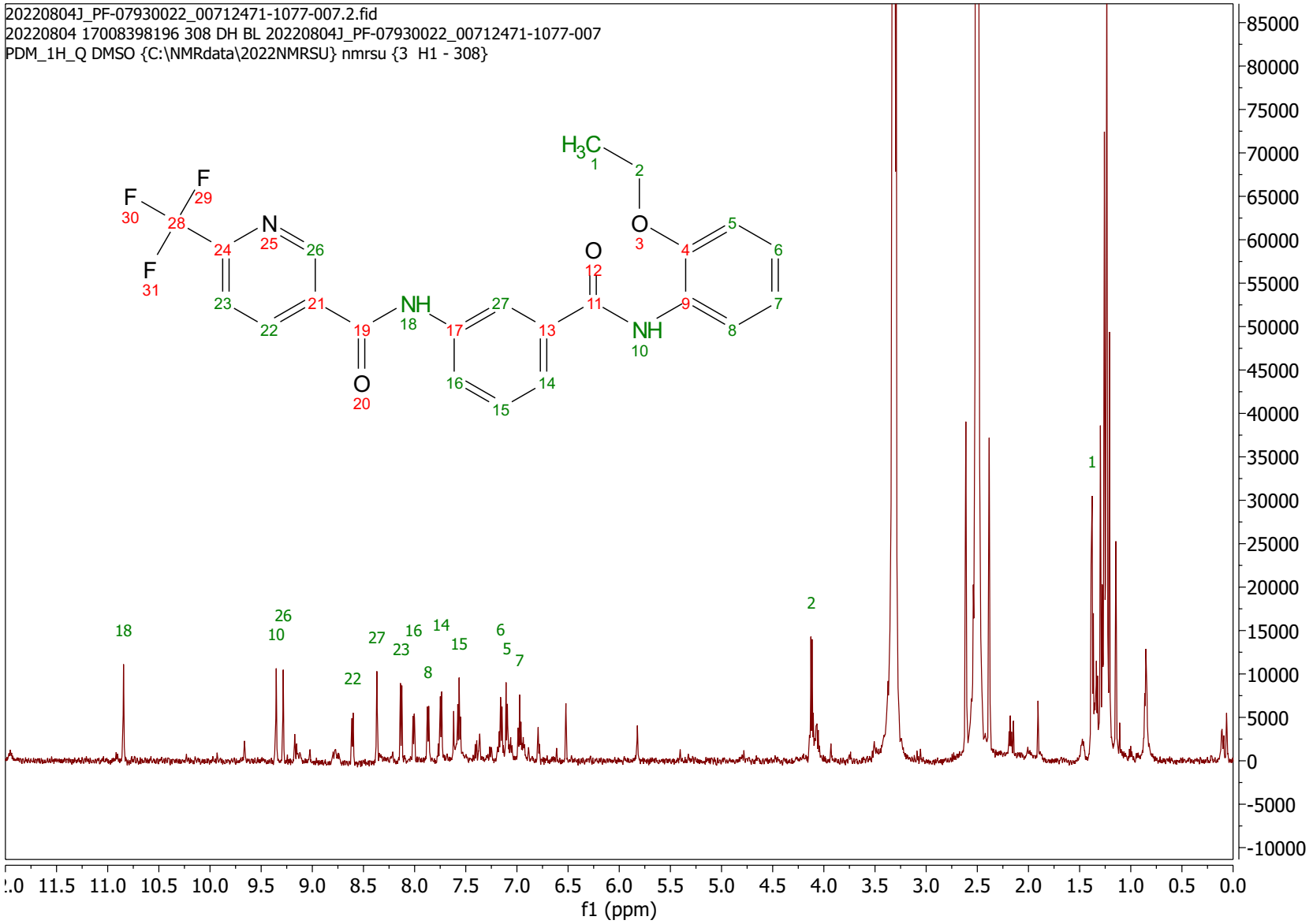
20220804J_PF-07930022_00712471-1077-007.2.fid
20220804 17008398196 308 DH BL 20220804J_PF-07930022_00712471-1077-007
PDM_1H_Q DMSO {C:\NMRdata\2022NMRSU} nmrsu {3 H1 - 308}
f1 (ppm)

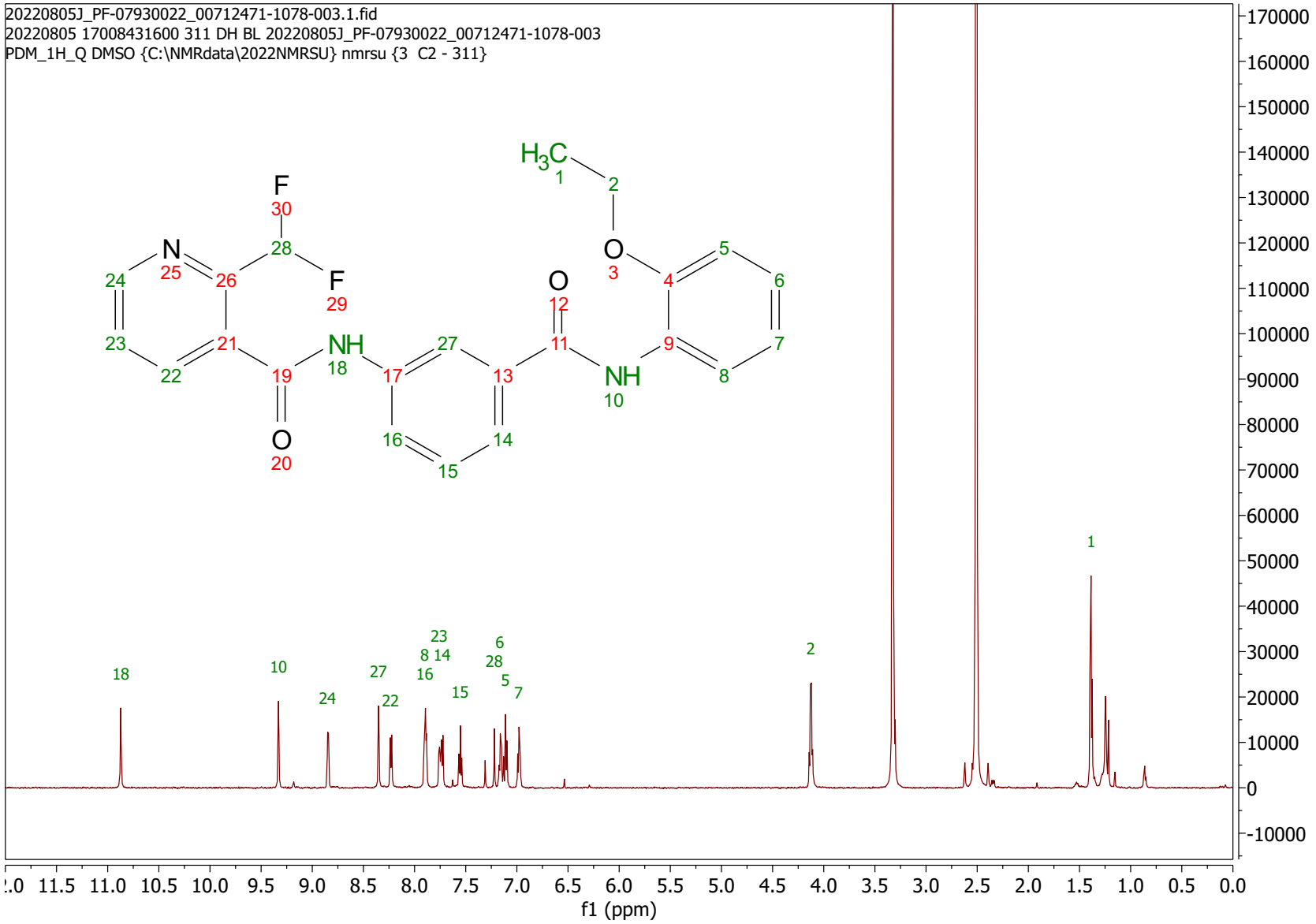
20220805J_PF-07930022_00712471-1078-003.1.fid
20220805 17008431600 311 DH BL 20220805J_PF-07930022_00712471-1078-003
PDM_1H_Q DMSO {C:\NMRdata\2022NMRSU} nmrsu {3 C2 - 311}
f1 (ppm)

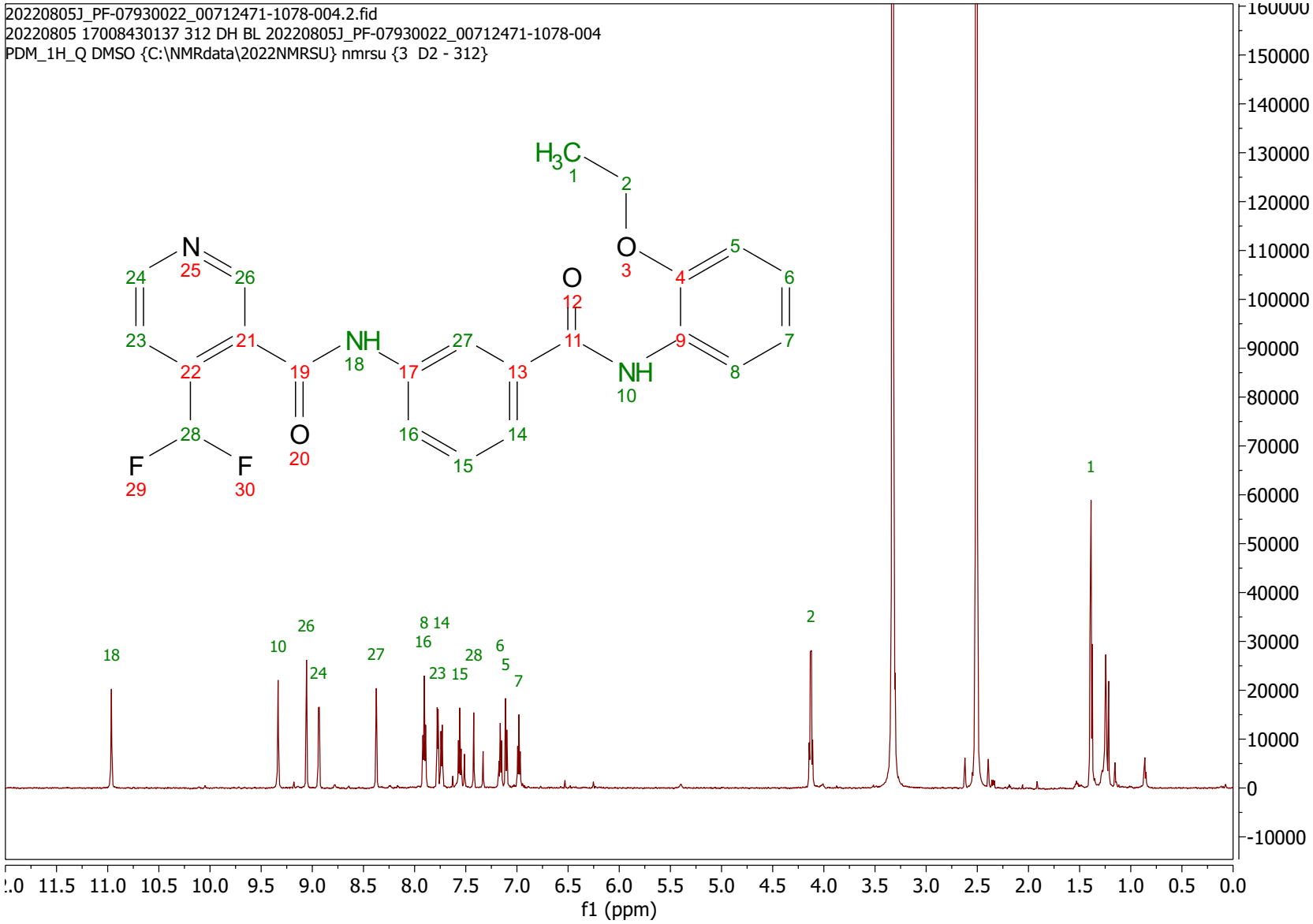
20220805J_PF-07930022_00712471-1078-004.2.fid
20220805 17008430137 312 DH BL 20220805J_PF-07930022_00712471-1078-004
PDM_1H_Q DMSO {C:\NMRdata\2022NMRSU} nmrsu {3 D2 - 312}
f1 (ppm)

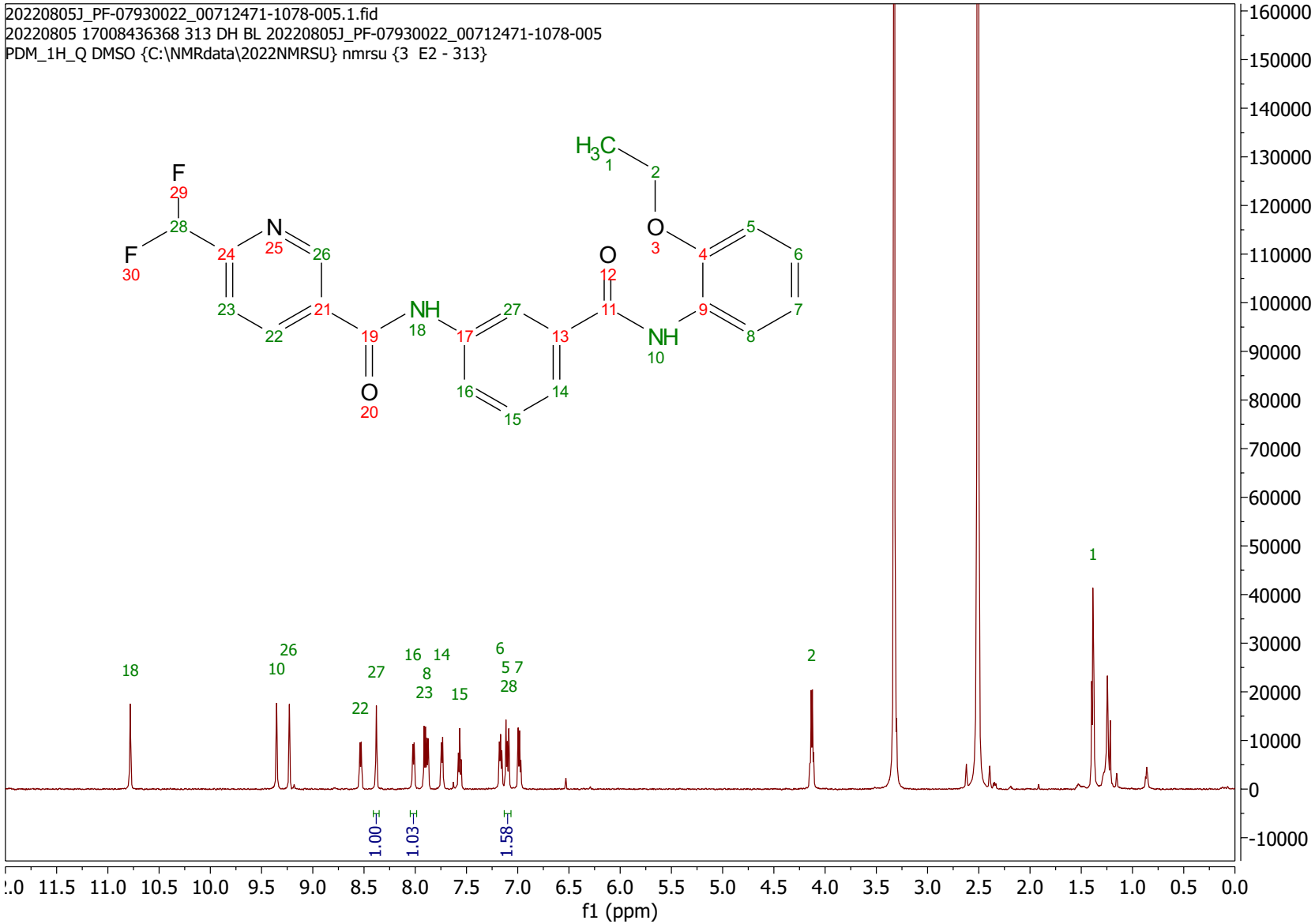
20220805J_PF-07930022_00712471-1078-005.1.fid
20220805 17008436368 313 DH BL 20220805J_PF-07930022_00712471-1078-005
PDM_1H_Q DMSO {C:\NMRdata\2022NMRSU} nmrsu {3 E2 - 313}
f1 (ppm)

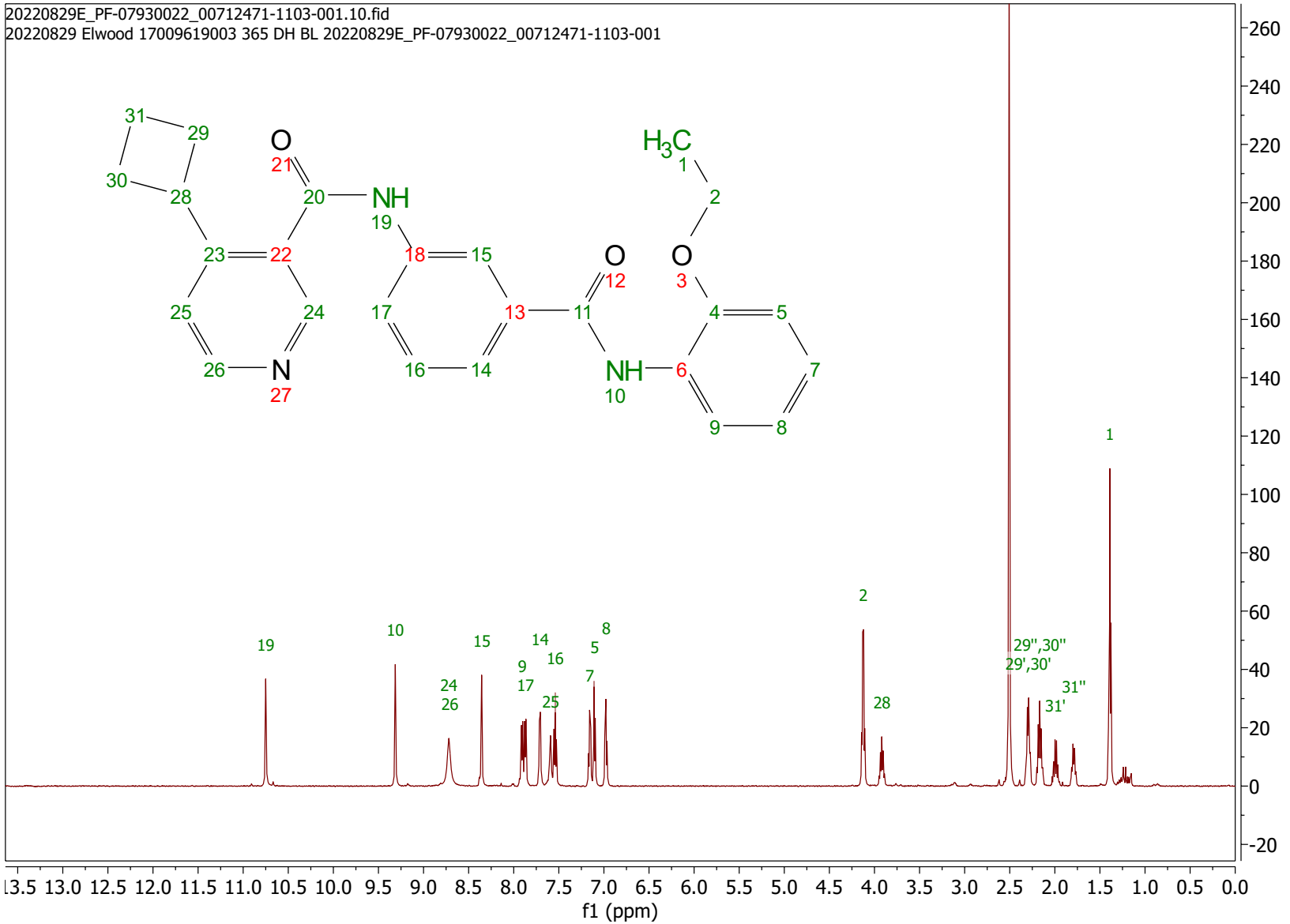
20220829E_PF-07930022_00712471-1103-001.10.fid
20220829 Elwood 17009619003 365 DH BL 20220829E_PF-07930022_00712471-1103-001
f1 (ppm)

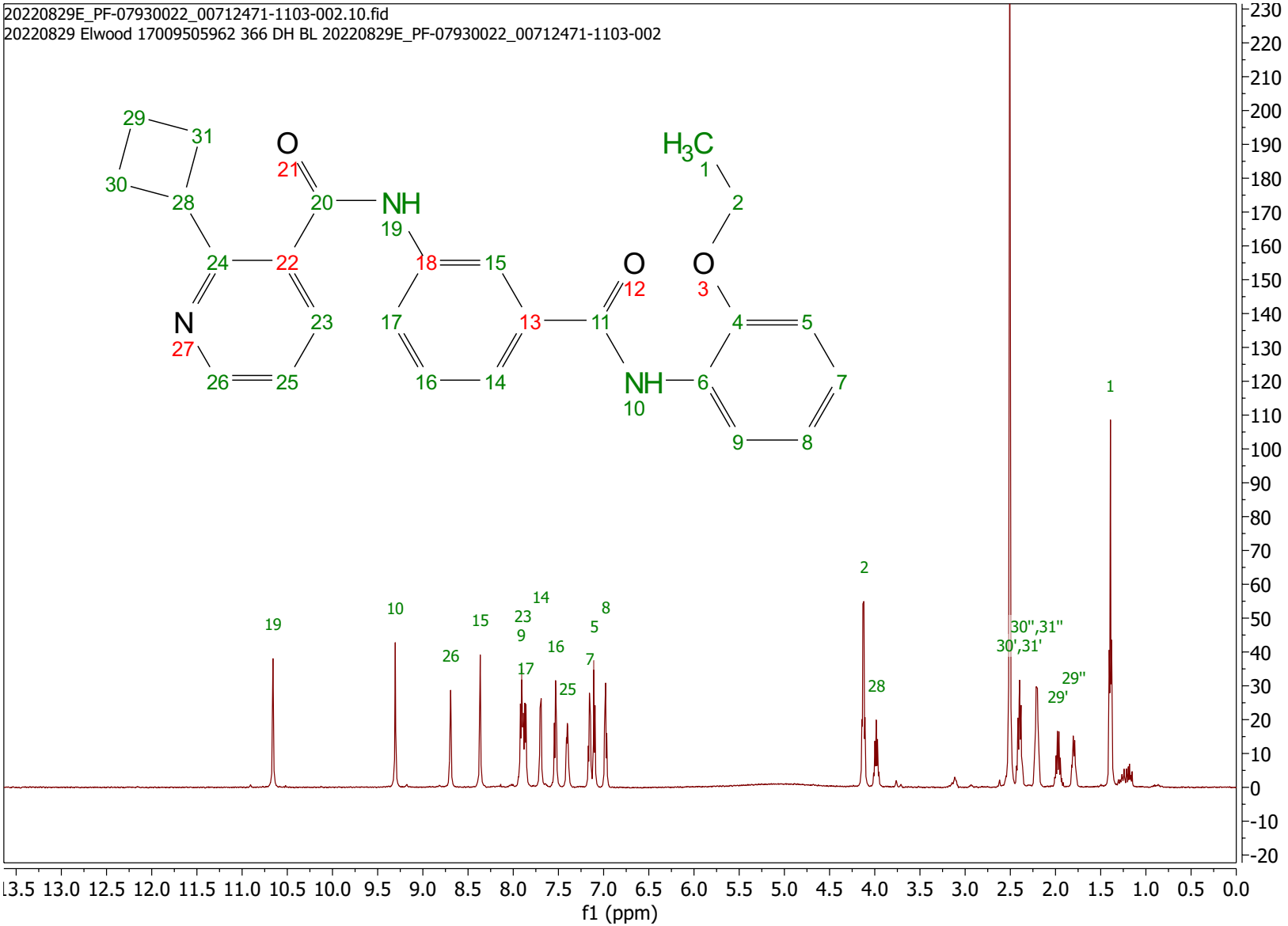
20220829E_PF-07930022_00712471-1103-002.10.fid
20220829 Elwood 17009505962 366 DH BL 20220829E_PF-07930022_00712471-1103-002
f1 (ppm)

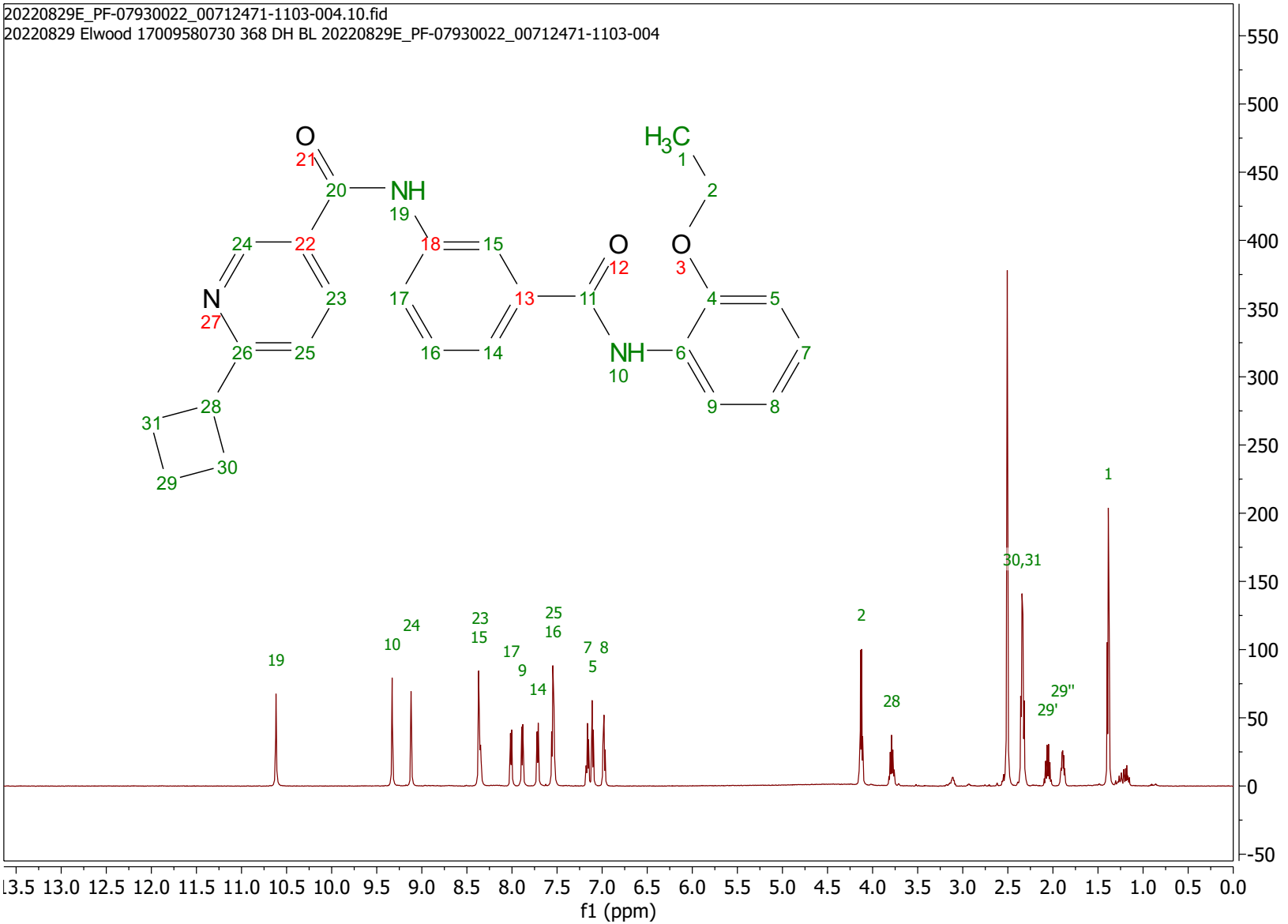
20220829E_PF-07930022_00712471-1103-004.10.fid
20220829 Elwood 17009580730 368 DH BL 20220829E_PF-07930022_00712471-1103-004
O
21
20
NH
19
24
22
18
15
O
12
O
3
H3C
1
2
N
27
23
17
13
11
4
5
26
25
16
14
NH
10
6
7
9
8
28
31
29
30
19
10
24
23
15
17
9
14
25
16
7
8
5
2
28
30,31
29'
29''
1
f1 (ppm)

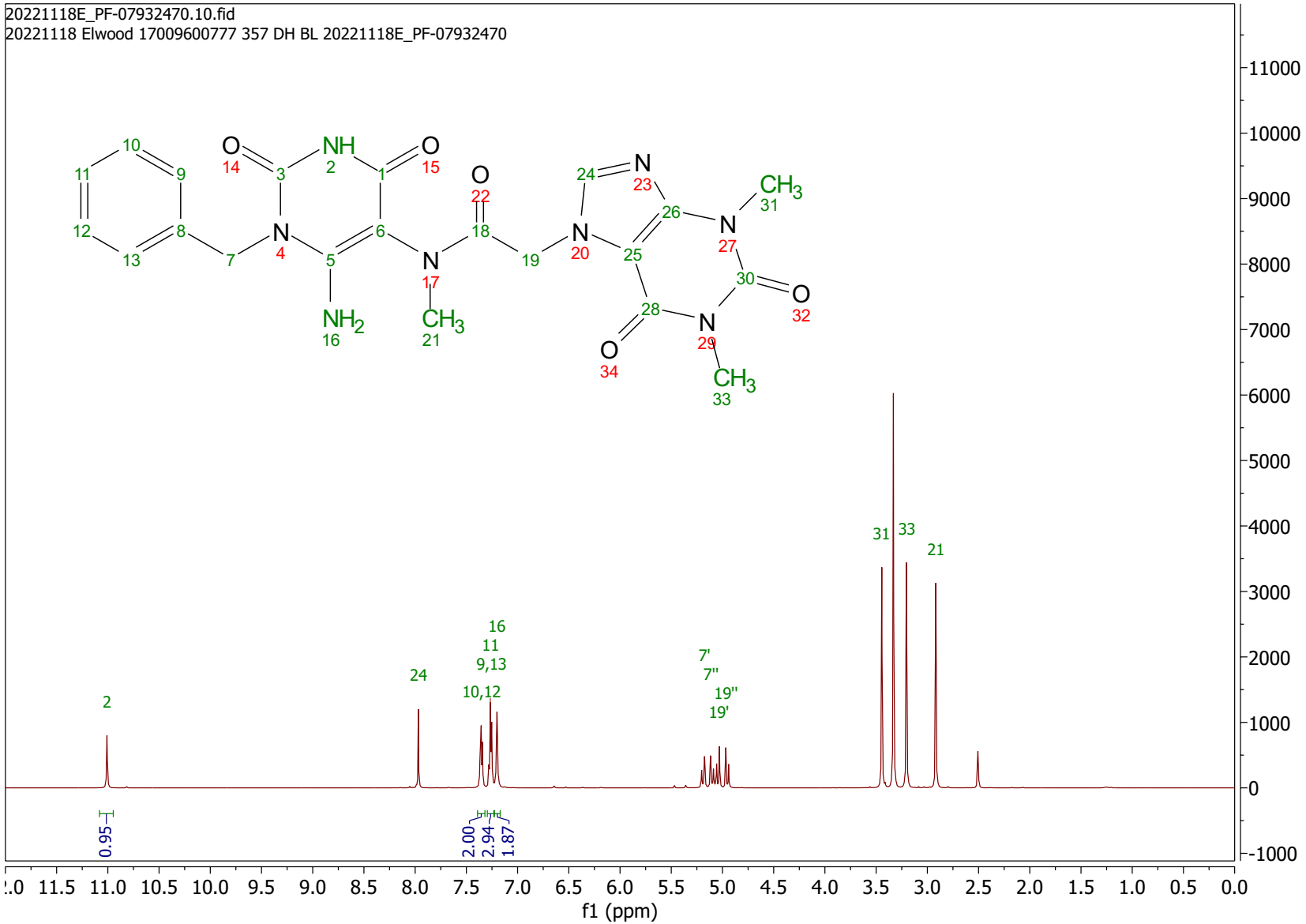
20221118E_PF-07932470.10.fid
20221118 Elwood 17009600777 357 DH BL 20221118E_PF-07932470
f1 (ppm)

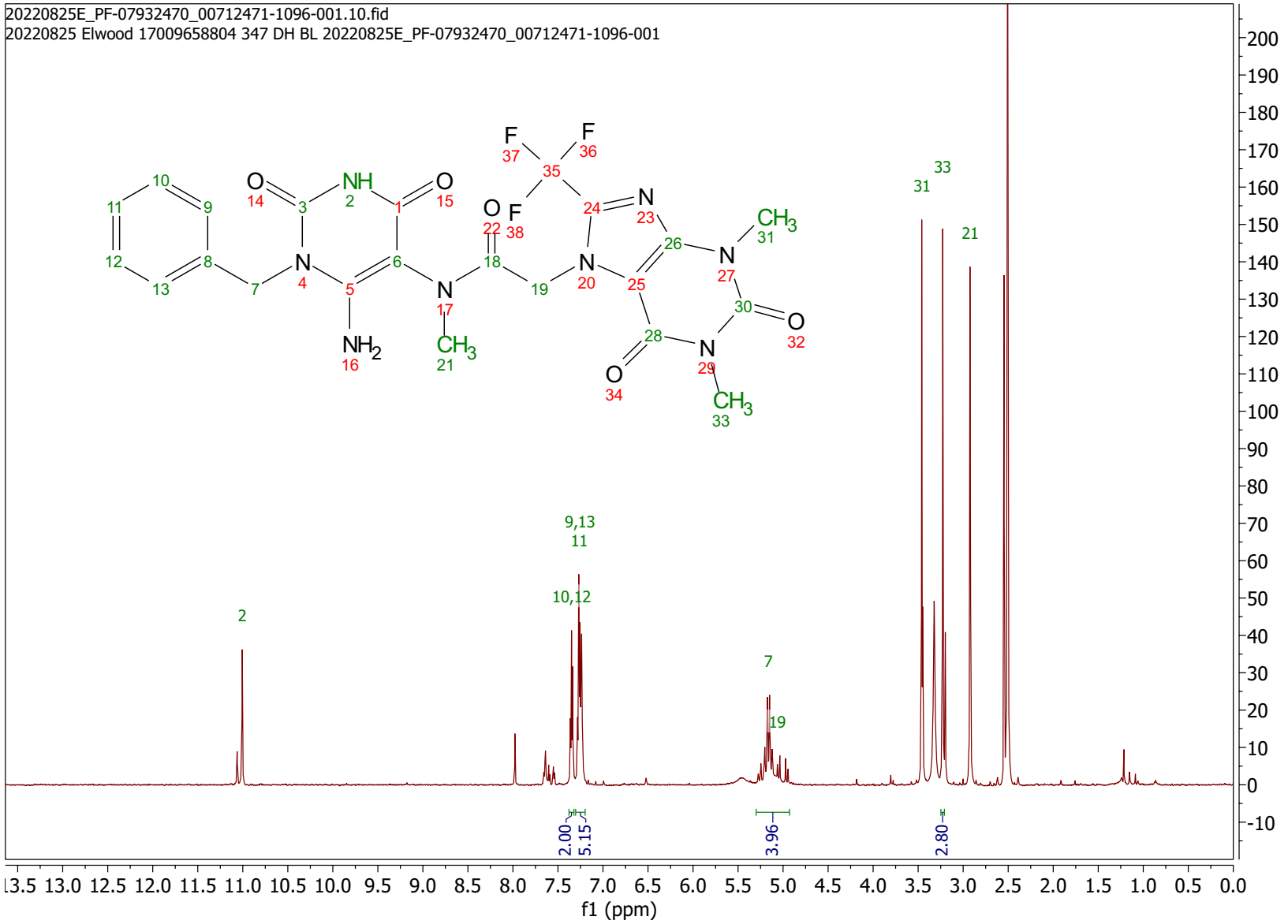
20220825E_PF-07932470_00712471-1096-001.10.fid
20220825 Elwood 17009658804 347 DH BL 20220825E_PF-07932470_00712471-1096-001
9,13
11
10,12
2
7
19
31
33
21
2.00
5.15
3.96
2.80
f1 (ppm)

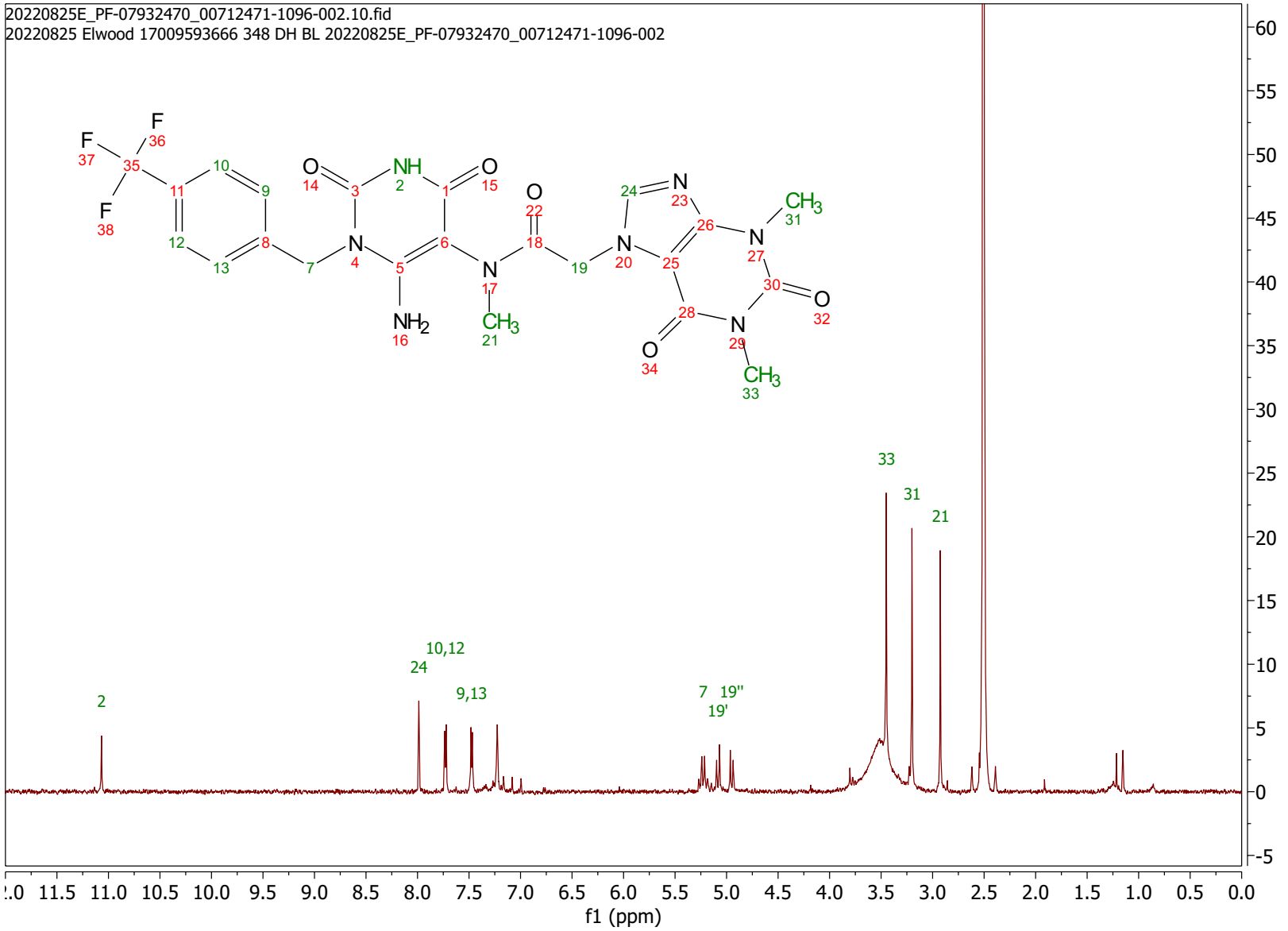
20220825E_PF-07932470_00712471-1096-002.10.fid
20220825 Elwood 17009593666 348 DH BL 20220825E_PF-07932470_00712471-1096-002
F
F
F
O
NH
O
O
N
N
N
N
N
O
O
O
O
NH2
CH3
CH3
CH3
2
10,12
24
9,13
7
19''
19'
33
31
21
f1 (ppm)

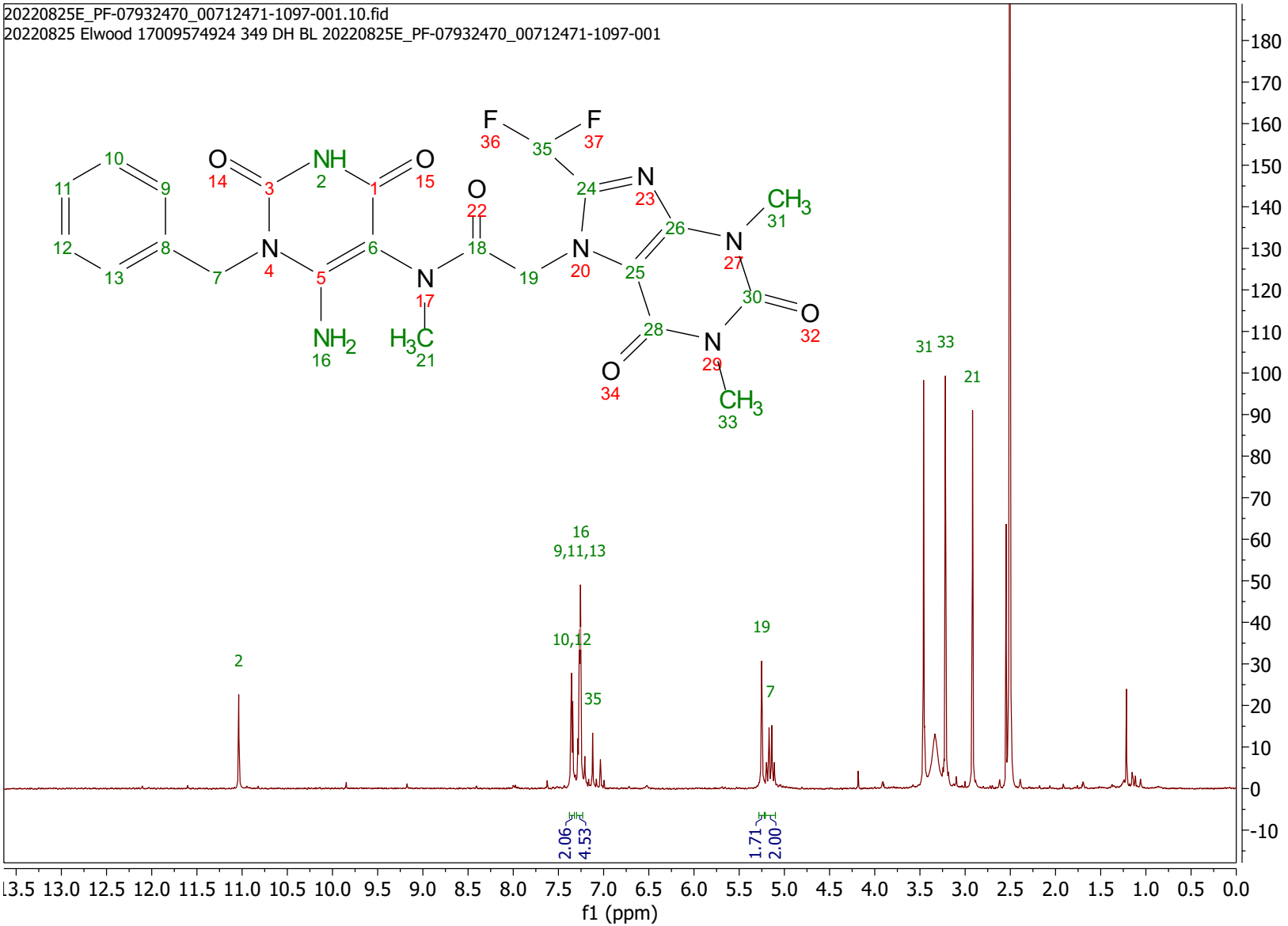
20220825E_PF-07932470_00712471-1097-001.10.fid
20220825 Elwood 17009574924 349 DH BL 20220825E_PF-07932470_00712471-1097-001
f1 (ppm)

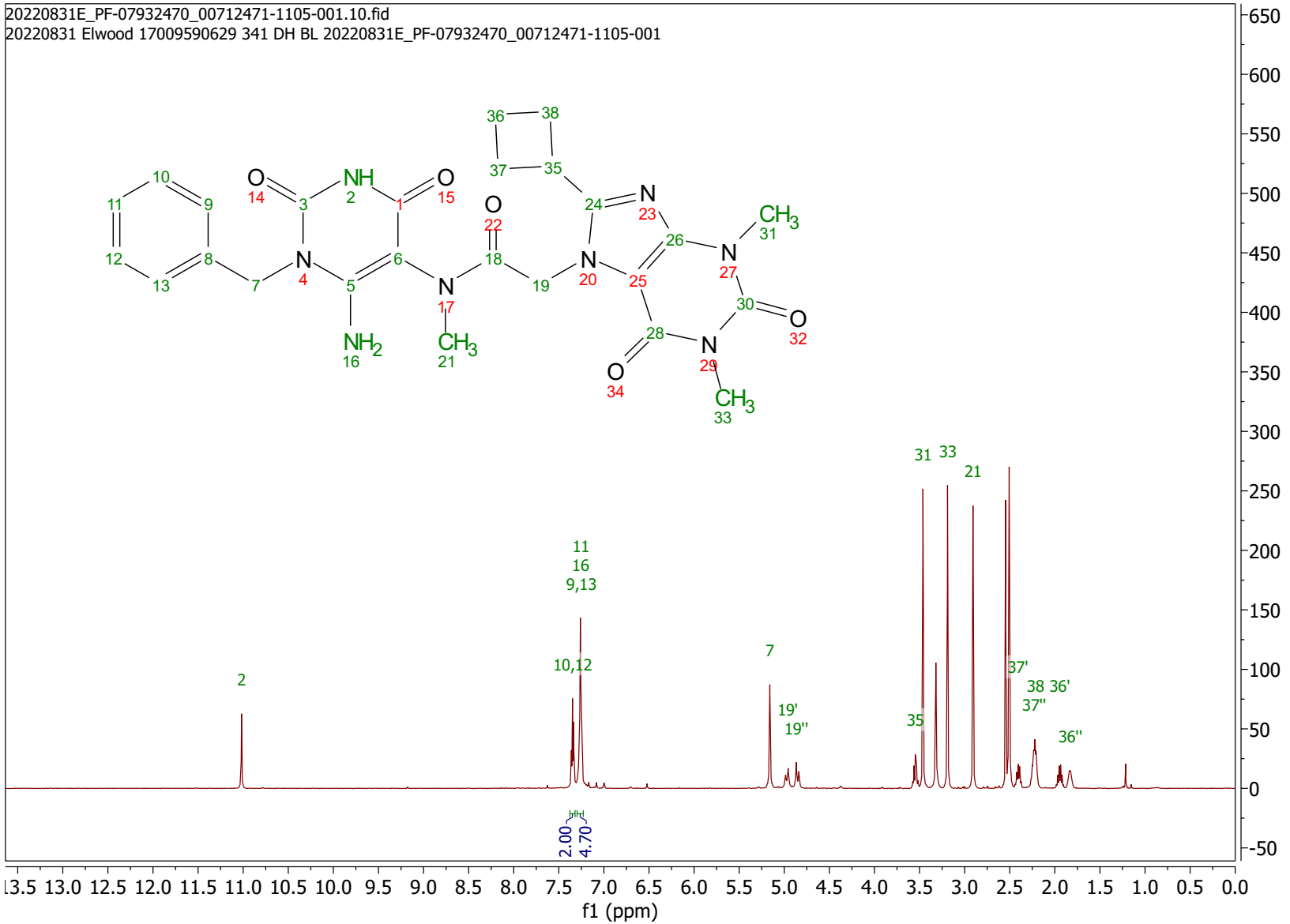
20220831E_PF-07932470_00712471-1105-001.10.fid
20220831 Elwood 17009590629 341 DH BL 20220831E_PF-07932470_00712471-1105-001
2
11
16
9,13
10,12
7
19'
19''
31
33
21
35
37'
38
36'
37''
36''
2.00
4.70
f1 (ppm)